$Si(p,\alpha)$ Total Reaction Cross Sections For Micro-Electronic Applications

By

Gerry R. Maughan

A Thesis Submitted To

The Faculty of Graduate Studies

University of Manitoba

In Partial Fulfilment

Of The Requirements For The Degree

Master of Science

July 1982

SI (ρ,α) TOTAL REACTION CROSS SECTIONS FOR MICRO-ELECTRONIC APPLICATIONS

BY

GERRY R. MAUGHAN

A thesis submitted to the Faculty of Graduate Studies of the University of Manitoba in partial fulfillment of the requirements of the degree of

MASTER OF SCIENCE

ABSTRACT

The ^{27}Al and natural silicon (p,α) total cross sections have been measured at proton energies of 35 and 45 MeV. The accuracy of the measurements is much better than that of previous measurements. The $(p, {}^{3}He)$ total cross sections have been measured with similar targets and energies. The primary motivation for obtaining these cross sections comes from micro-electronic applications. When the nucleon component of the cosmic ray flux interacts with the silicon in computer memory chips, the resulting highly ionizing particles can cause memory errors. These measurements along with measurements from the literature show the energy dependence of the (p,α) cross section. This energy dependence was convoluted with the cosmic ray flux to determine an upper limit for the failure rate due to cosmic ray sources. The angular distributions of the (p,α) differential cross sections were also obtained.

ACKNOWLEDGEMENTS

I would like to thank Dr. W.T.H. van Oers and Dr. R.H. McCamis for the help and supervision that they provided throughout this project. They along with Dr. N.E. Davison, Dr. J.P. Svenne and Dr. H.C. Card are thanked for serving on my committee.

Also J.R. Anderson, C.A. Smith, J.R. Campbell and P. Beaulieu contributed to the computer programming. Many people including some of the above helped me by doing shifts on the cyclotron. In addition, the machine shop, the electronics shop, the cyclotron office and the physics office personnel were all called upon at various times and their co-operation is appreciated.

TABLE OF CONTENTS

List of Figures

List of Figures (cont.)

List of Tables

CHAPTER I

INTRODUCTION

Relevance to Micro-electronic Technology

The primary purpose for measuring the total reaction cross section for alpha particle production by protons on silicon is related to the effect that cosmic rays have on computer memories. As explained by J.F. Ziegler and W.A. Lanford[1] the maximum charge density developed by the ionization wake of alpha particles in silicon is 70,000 e^- per micrometer over path lengths of about 7 μm at the end of their range. Since 1978 electronic circuit components have been made small enough that they are sensitive to these bursts. An impinging alpha particle can cause the spontaneous flipping of a single binary bit and thus cause an error in an otherwise correctly functioning computer memory chip. Although it is not totally relevant to the present treatise it should be pointed out that some chips are now small enough to become sensitive to proton and muon ionization wakes.

Ziegler and Lanford point out that these error-causing alpha particles can come from two sources. They can be produced by nearby trace uranium and thorium concentrations or they can be produced by the nucleon component of cosmic rays. Because of their relative concentrations cosmic ray neutrons are more important than protons at sea level and cosmic ray protons increase in significance with elevation. Clearly in order to estimate the magnitude of the effect of cosmic rays on computer memories a knowledge of the Si (p,α) and Si (n,α) total reaction cross sections is essential.

Figures 1-1 and 1-2 from reference 1 show average cosmic ray fluxes of the various particles for 45°N latitude at sea level and at 3 and 10 km elevations. Our measurements at 35 and 45 MeV are just to the left of the broad cosmic ray proton peak which is centred at about 100 MeV so our energy range is certainly important.

Existing Measurements

Figures 1-3 and 1-4 show the existing (p,α) total cross sections for silicon and nearby aluminum in the relevant energy range. Measurements of the ^{27}Al and Si (p,α) total cross sections have been made between 16 and 45 MeV by Walton et al[2]. The ^{27}Al (p,α) cross sections have also been measured at 23 MeV by Fulmer and Cohen,[3] at 62 MeV by Bertrand and Peele[4] and at 90 MeV by Wu, Chang and Holmgren.[5] Measurements at 165 MeV have been planned at the Indiana University Cyclotron Facility[6] while measurements of the ^{27}Al (p,α) cross sections have been made at an intermediate energy of 0.6 GeV by Alard et al[7] and 2.1 and 4.9 GeV by Westfall et al.[8] The Al (p,α) cross section at 62 MeV had a cutoff energy of 2.9 MeV so the total cross section will be slightly higher than shown.

Ziegler and Lanford[6] point out that the Walton et al[2] measurements show a large variation with energy and a large variation between silicon and aluminum. New measurements at 35 and 45 MeV are thus needed from the point of view of fundamental nuclear physics to resolve this low energy anomaly. These new measurements along with the existing high energy measurements will give the energy-dependence of the Si (p,α) total cross section. By inference the (n,α) total cross sections can be obtained and thus an upper limit to the highly ionizing alpha particles (due to cosmic rays penetrating micro-electronic silicon chips) will be known. These data will be useful in future micro-electronic research and design.

Fig. 1-1 Cosmic Ray Flux At Sea Level
Taken from Reference (1)

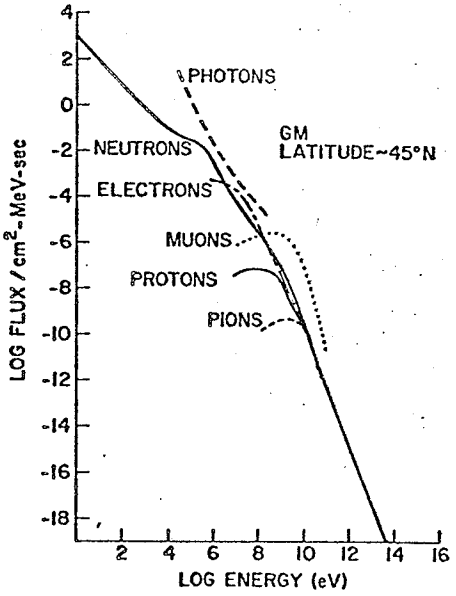

Flux of cosmic-ray particles at sea level. The curves are average values and large fluctuations exist that are attributed to magnetic latitude, time of day, season, solar cycle, angle of incidence, and so on. Geomagnetic (*GM*) latitude 45°N was chosen because of the availability of extensive experimental data. The muon flux is for μ^- particles; the total muon flux ($\mu^- + \mu^+$) is 2.29 times this value.

Fig. 1-2 Cosmic Ray Flux At 3 And 10 km Altitude
Taken from Reference (1)

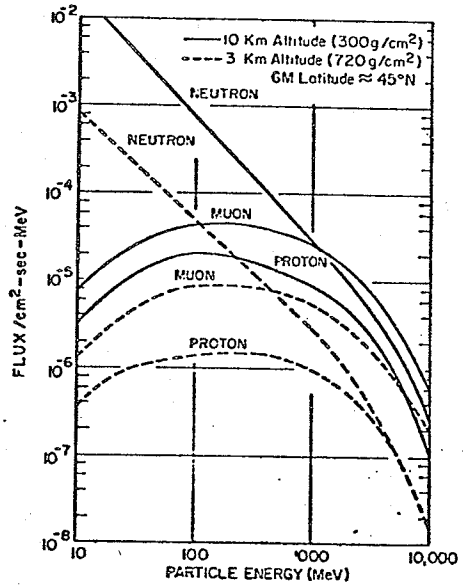

Experimentally determined cosmic-ray fluxes at altitudes of 3 and 10 km at about geomagnetic latitude 45°N.

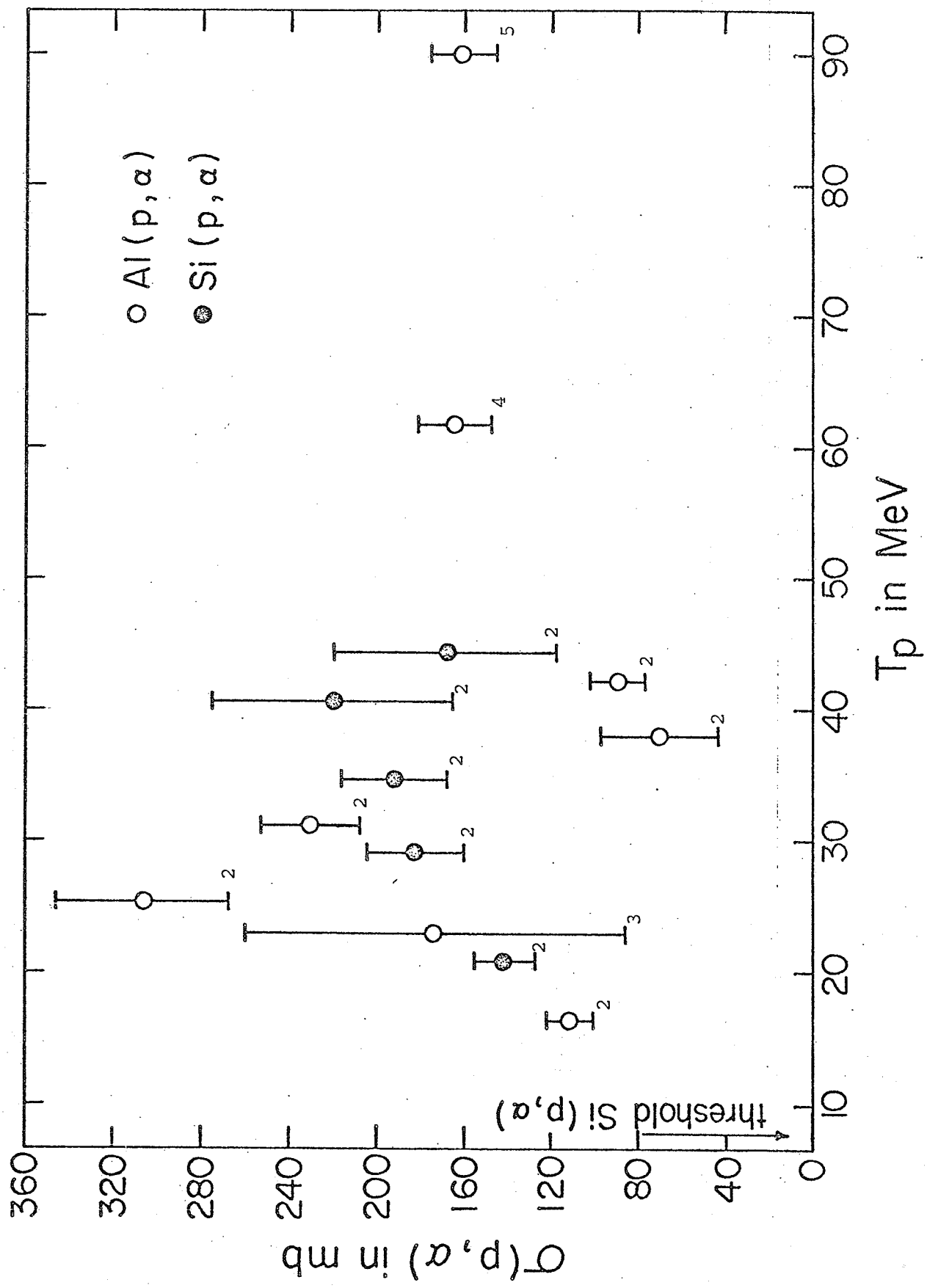
σ(p,α) in mb
Tp in MeV
o Al(p,α)
● Si(p,α)
threshold Si (p,α)
0
40
80
120
160
200
240
280
320
360
10
20
30
40
50
60
70
80
90

Fig. 1-3

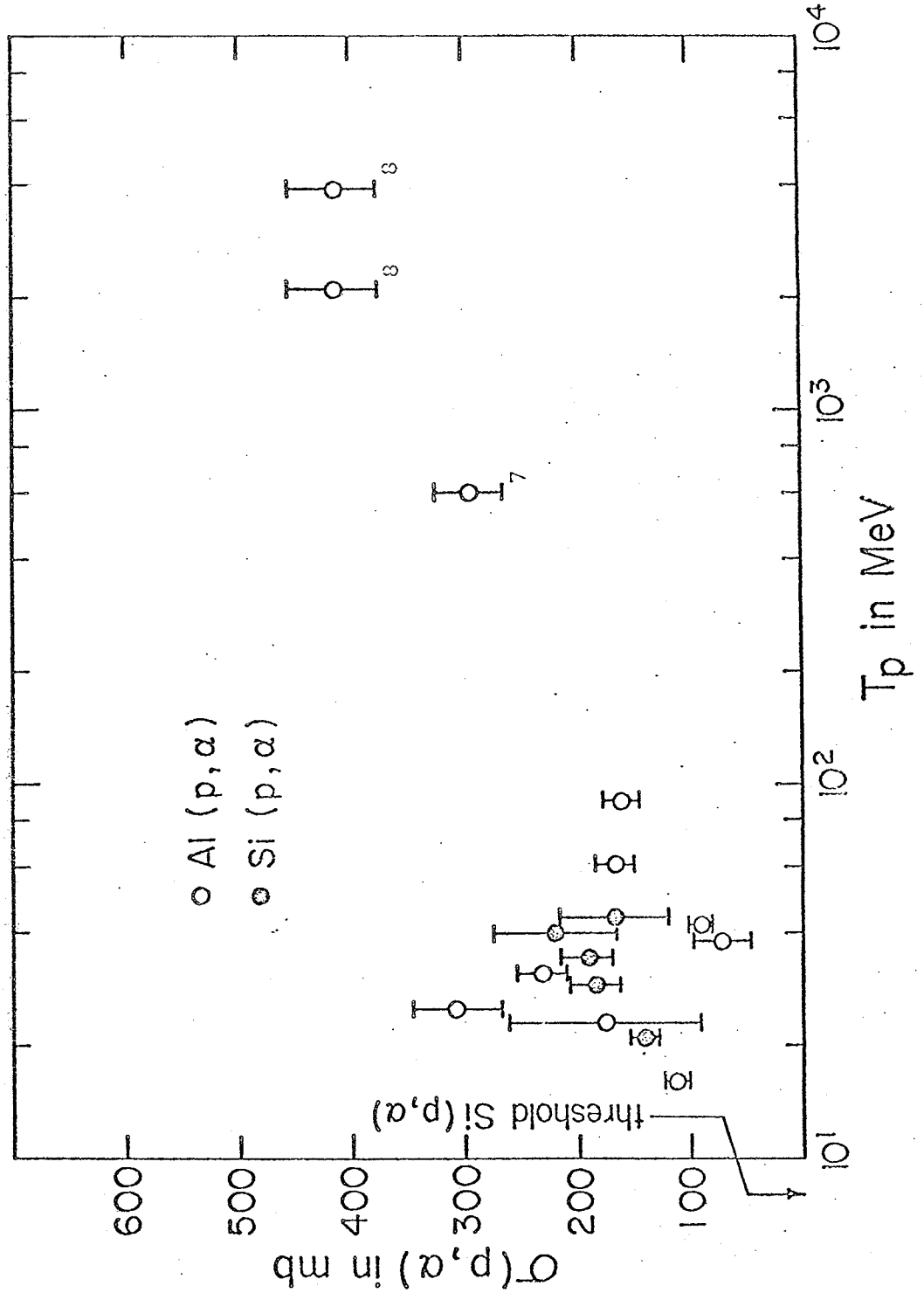
σ(p,α) in mb
600
500
400
300
200
100
threshold Si (p,α)
10¹
10²
10³
10⁴
Tp in MeV
o Al (p,α)
• Si (p,α)
8
8
7

Fig. 1-4

Astrophysical Importance

Walton et al[2] point out that these measurements also have astrophysical importance. Seventy percent of the solar cosmic rays are made up of protons of energies generally less than 50 MeV. When these particles hit bodies without an atmosphere such as the moon, they interact with the top few centimeters of soil and produce new elements by nuclear reactions. These new elements have different isotopic abundances from those produced by galactic cosmic rays because the energy of the solar cosmic ray particles is generally smaller. Thus valuable information on the history and evolution of lunar soils may be uncovered with the help of these cross section measurements.

CHAPTER II

MEASUREMENTS

Cyclotron Facilities

Figure 2-1 is a diagram of the experimental area at the University of Manitoba Cyclotron. The beam lines which go to experimental room B are not shown for clarity. The experiments were done in the 71 cm. diameter scattering chamber in experimental room A on the 45 degree right beam line. The incident energy of the beam was known to ±250 keV, while the beam energy spread was estimated to be 200 keV FWHM. Beam intensity on target was about 10 nA except when measuring very forward angles where it was decreased (to 1 nA at 15^{o}) in order to prevent damaging the detectors.

After two set-up experiments final data were taken of the ^{27}Al and natural Si (p,α) total cross sections, at 35 and 45 MeV, in two runs each using about five days of beam time.

Downstream of the scattering chamber a Faraday cup sent a signal of the total amount of charge collected to a Brookhaven Instruments Corporation current integrator and digitizer which provided an output for a scaler. The relationship of one count equals 2×10^{-1} n coul. was used to calculate the total number of incident protons for each run. The charge integrator had an accuracy of 0.1% for its digitized output. The proton beam generally had a "halo" of an undetermined dimension. Past experience has shown that the halo, which may not entirely be collected in the Faraday cup represents <1% of the total proton cross section. An overall uncertainty of 1% was therefore assigned to the charge integration.

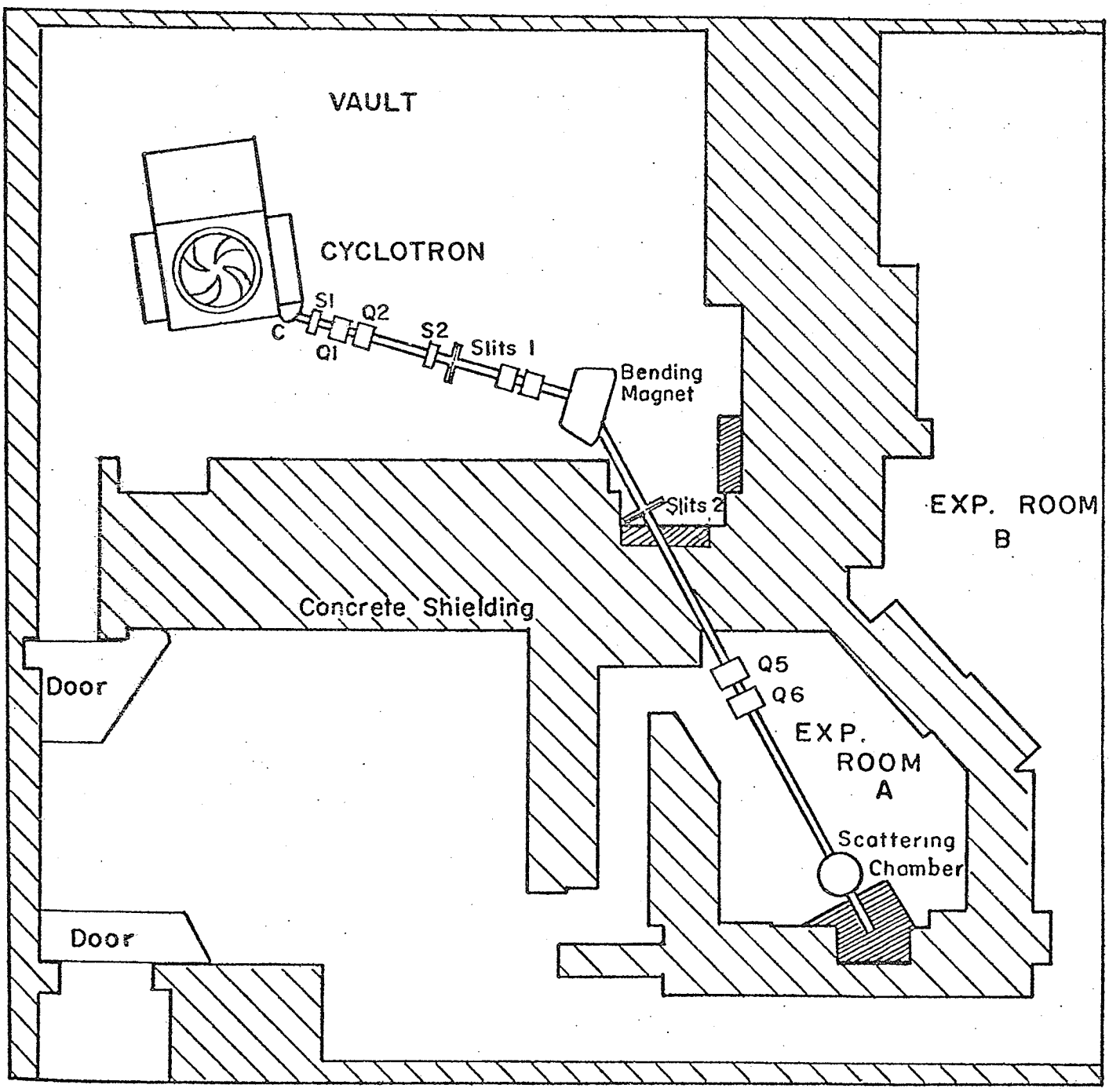

Fig. 2 - 1 Cyclotron Beam Line Layout.

The beam line and chamber were kept at a vacuum of less than 2×10^{-5} torr. during all data taking runs.

The Scattering Chamber

A diagram of the 71 cm scattering chamber is shown in Figure 2-2. The target position is in the exact centre of the chamber. The detectors were kept in plastic holders in brass cubicles in order to shield them from stray currents and electric fields and thus keep the noise levels low. These cubicles were mounted one on each of the two moveable tables which rotate around the chamber centre. Digitized angular controls for these tables were located in the control room so that detector positions could be checked during a run or changed remotely at any time.

Two NaI monitors were located at 37.5 degrees left and right with respect to the zero degree axis of the chamber. These were set up to count elastically scattered protons. Thus if the beam drifted to one side during a run then this would be detected by one monitor counting significantly higher than the other. The ratios of elastically scattered protons in these monitor detectors were kept to 1.00 ± 0.02.

Measurements were taken in five degree steps from 15 to 50 degrees, in ten degree steps from 60 to 150 degrees and at 165 degrees. The forward and backward angle measurements were taken with the left and right detectors at identical angles and with the target perpendicular to the beam. For the medium angle measurements (60 to 120 degrees) the target ladder was rotated 45 degrees and the left and right detectors were placed directly opposite each other. For instance if the left detector was at 70 degrees then the right would be set to 110 degrees. Height notches and an angle indicator were located on the target ladder enabling target position and angle to be set to within $\pm$ 0.5 percent.

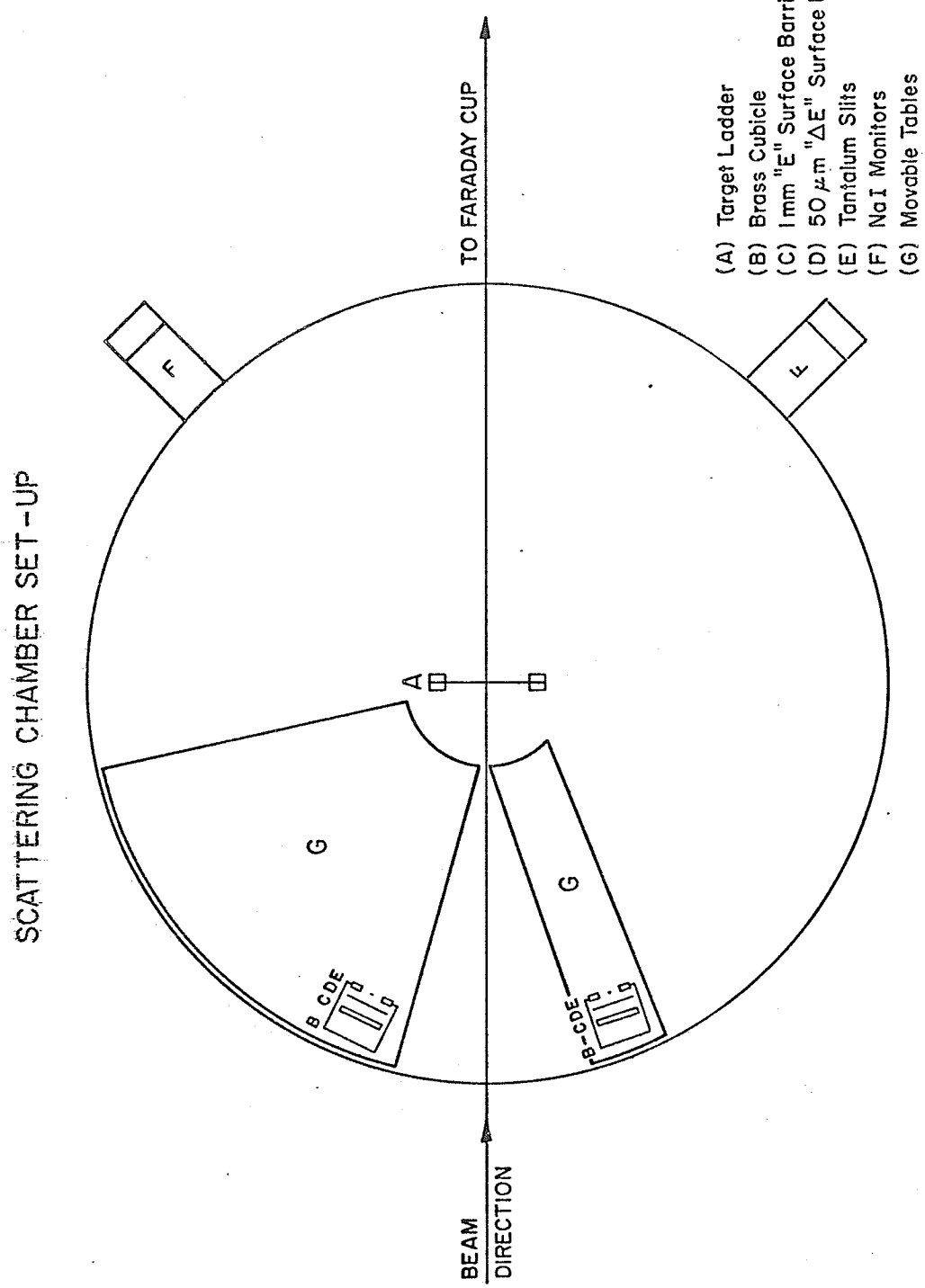
SCATTERING CHAMBER SET-UP
TO FARADAY CUP
BEAM
DIRECTION
A
B CDE
B-CDE
G
G
F
F
(A) Target Ladder
(B) Brass Cubicle
(C) 1mm "E" Surface Barrier
(D) 50 μm "ΔE" Surface Barrier
(E) Tantalum Slits
(F) NaI Monitors
(G) Movable Tables

Fig. 2-2

The Targets

The aluminum target consisted of a foil which was 2.28 ± 0.005 mg/cm^2 (or 8.46 μm) thick. A thin silicon target was more difficult to obtain so a decision to use a radiation damaged surface barrier detector was made. The one chosen was 100 mm^2 in area and 9.32 ± 0.02 mg/cm^2 (or 40 μm) thick. Whereas the aluminum foil was composed of essentially 100 percent ^{27}Al, the silicon target was composed of natural silicon which contains 92.21 percent ^{28}Si, 4.70 percent ^{29}Si and 3.09 percent ^{30}Si. The silicon used for most electronic applications has these same proportions. In addition the silicon target had two thin electrical contacts on its surfaces, the front one being gold and the back one being aluminum. Each was 10 μg/cm^2 thick as specified by the manufacturer. A calculation showed that this was thin enough that relative to the experimental errors in this experiment the electrical contacts could be totally neglected.

Because of the unusual dimensions of the silicon target a special target ladder had to be designed and built. Careful measurements were taken to ensure that the surface of the detector would be in the exact centre of the scattering chamber so that all angular measurements would be correct. The target ladder had three-positions so one could change from silicon to aluminum to the fluorescent screen without venting the chamber. The screen was used to centre and focus the beam to a size which was kept smaller than a 3 mm diameter circle.

Because the silicon target was a fairly small detector a dummy target with the same outside dimensions but with the silicon wafer removed was made. Measurements were then taken with this dummy target to ensure that the background from scattering from the edges was negligible.

Initially it was not known what the silicon and aluminum spectra would look like so a CH_2 target was used for set-up purposes to produce spectra which were seen to be satisfactory in shape and resolution.

The Collimators

The collimators were made from tantalum because of its high proton stopping power. Thus the collimators could be made relatively thin to reduce the problem of particles scattering off the inside of the slits into the detectors. For the 35 MeV run collimators 2.315 $\pm$ 0.01 mm thick were used and for the 45 MeV run 2.795 $\pm$ 0.01 mm collimators were used. These thicknesses ensured that the highest energy elastically scattered protons in each case would be stopped. The collimators were mounted onto the brass cubicles.

Each slit was approximately eleven mm high by five and a half mm wide. Careful measurements of the apertures of the collimators were made. A travelling microscope was used to measure the slit width in at least four places, the slit height in at least three places and the radius of the slit corners for each collimator. These resulted in an area of 59.5 $\pm$ 0.1 mm^2 for the left slit at 45 MeV and areas of 59.3 $\pm$ 0.1 mm^2 for the others.

The collimators were placed at 30.8 $\pm$ 0.1 cm from the target centre during the 45 MeV run and at 27.6 $\pm$ 0.1 cm during the 35 MeV run. The solid angle the collimators define is then given by the area of the slit divided by the square of the distance from the target. This equals 7.77 x 10^{-4} steradian for the 35 MeV collimators, 6.27 x 10^{-4} steradian for the left collimator at 45 MeV and 6.25 x 10^{-4} steradian for the right collimator at 45 MeV. The errors in the solid angles are one percent.

The Detectors

The detectors used were Ortec surface barrier detectors. The delta E detectors were 50 μm thick and 150 mm^2 in area and had a resolution of approximately 30 keV. The E detectors were 1 mm thick and 200 mm^2 in area and had similar resolutions. The delta E detector would stop any alpha

particle with energy less than 8 MeV. and the delta E and E detectors together could stop any alpha particle with less than 50 MeV. The leakage currents were routinely checked when the detectors were biased to ensure that they were operating correctly.

Electronics

A diagram of the electronics used is shown in Figure 2-3. All of the modules used were manufactured by Ortec. Figure 2-4 shows the pulse shapes and how the timing was set up at crucial locations.

For both left and right sides the delta E and E detector signals were sent through pre-amplifiers to spectroscopy amplifiers. The amplifiers' shaping times were set at 0.5 μs. The bipolar pulses from the spectroscopy amplifiers triggered the timing single channel analysers if above a set threshold. The resulting signals were sent to the coincidence unit. If the delta E and E signals arrived in coincidence then a signal was sent to the gating inputs of each linear gate to admit the unipolar pulses from delta E and E spectroscopy amplifiers. A signal from the coincidence unit was also used to trigger a scaler and to produce the strobe signal for the computer. The signal from the 93 Ω output of the delta E linear gate was sent directly through a delay amplifier to the ADC to give the delta E signal. The 1 Ω output from the two linear gates were then added together in a dual sum and invert amplifier and then fed through another dual sum and invert amplifier to make the pulses positive again. This produced the E total signal which was sent to the ADC. The timing and pulse duration times were adjusted so that the delta E and E total signals arrived at the ADC in coincidence and were 1 μs long. The strobe pulse was adjusted to arrive 0.5 μs before the end of the delta E and E total signals.

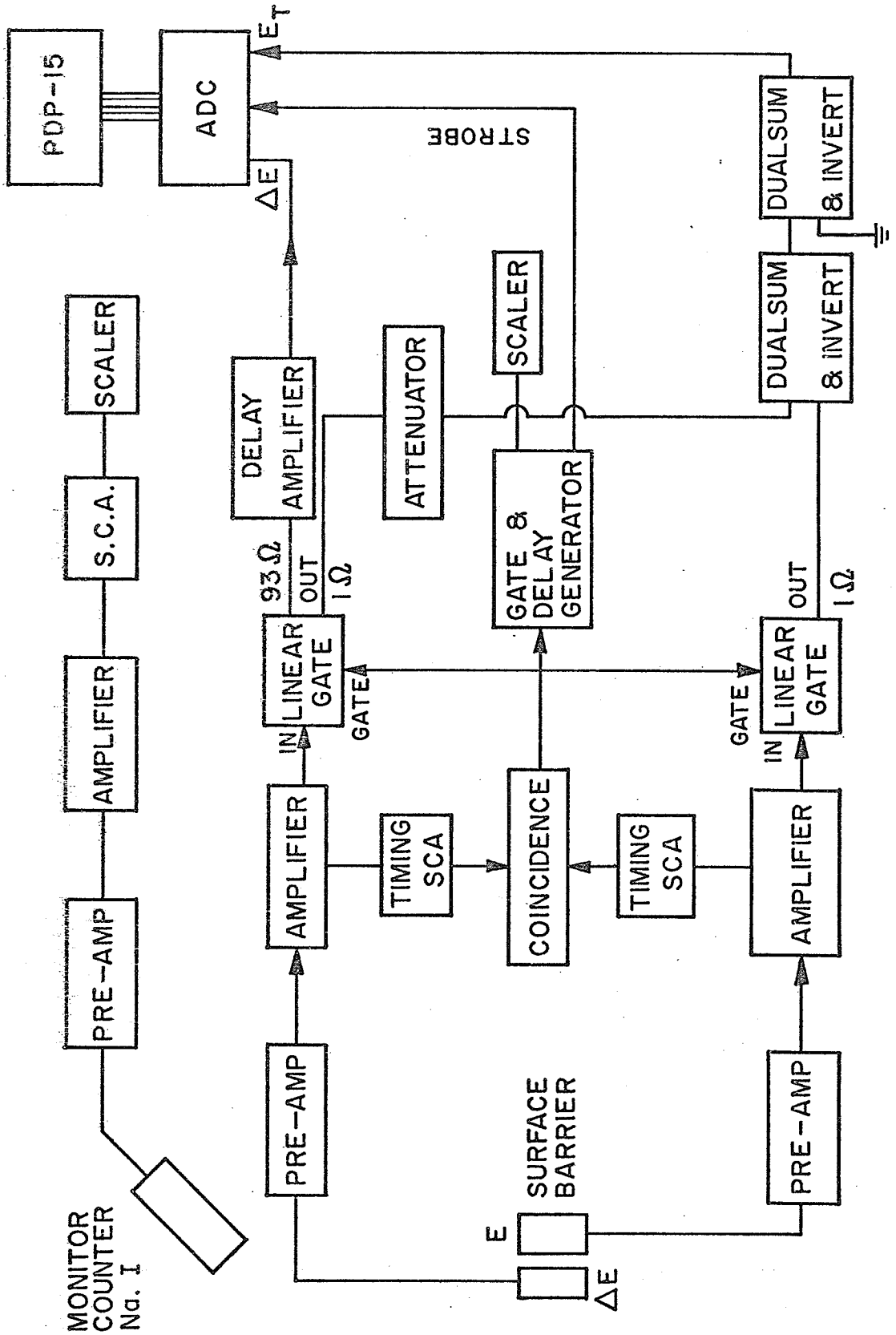

Fig. 2-3 DIAGRAM OF THE ELECTRONICS

PULSE SHAPE AND TIMING DIAGRAM

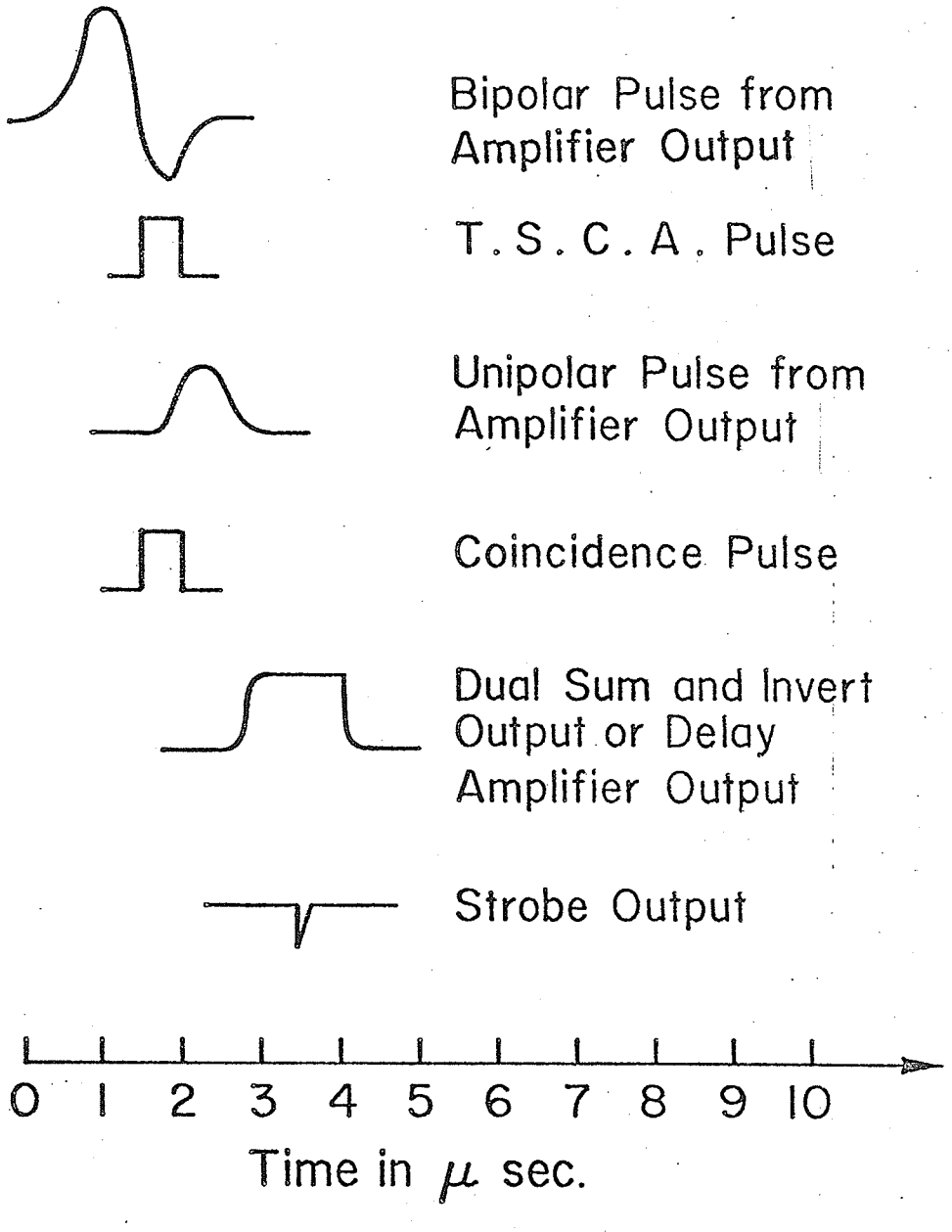

Fig. 2-4

Because the delta E and E signals were summed electronically to produce the E total signal the gain matching was very crucial. Figure 2-5 shows the electronics used to do the gain matching. The size of the pulses at various locations is also indicated. Initial set-up was done by passing a signal from a research pulser through the test inputs of the preamplifiers. In order to provide better resolution for the delta E - E total plots produced by the computer the delta E signal was amplified four times and then decreased by two 2X alternators just before being summed with the E signal in the first dual sum and invert unit.

Final gain matching was done by taking out the coincidence requirements and biasing the detectors. Then a pulser signal of 230 mV was sent through an Ortec charge terminator to each preamplifier and the spectroscopy amplifiers were adjusted in turn until the output pulses at the dual sum and invert were exactly 1.2 volts. Then beam was sent into the aluminum target and the spectroscopy amplifier outputs were checked on an oscilloscope for clipping. The aluminum target was used because it had the largest Q value so it produced the most energetic alpha particles. If clipping did occur then both spectroscopy amplifier gains were turned down proportionately until this problem was eliminated.

The next step was to check the two ADC's for linearity and to make sure that channel 0 corresponded to zero energy. The right signal went to a CAMAC ADC and the left signal went to a Northern NS 625 ADC. The pulser was sent to each detector system in turn and a graph of pulser gain versus channel number was made. In all cases the ADC's responses were linear but in some instances the zero point had to be adjusted. Figure 2-6 is an example of this.

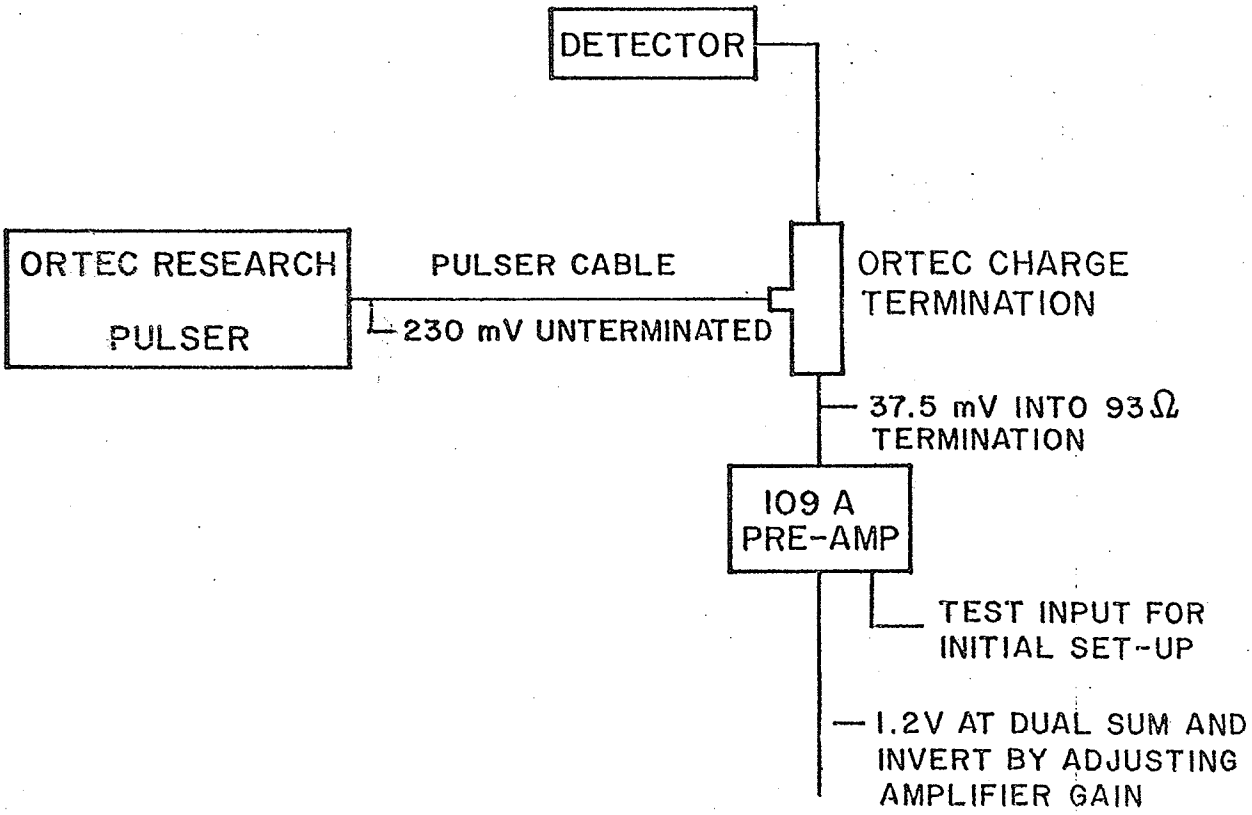

FIG. 2-5 GAIN MATCHING ELECTRONICS
(Pulse size is indicated at key locations)

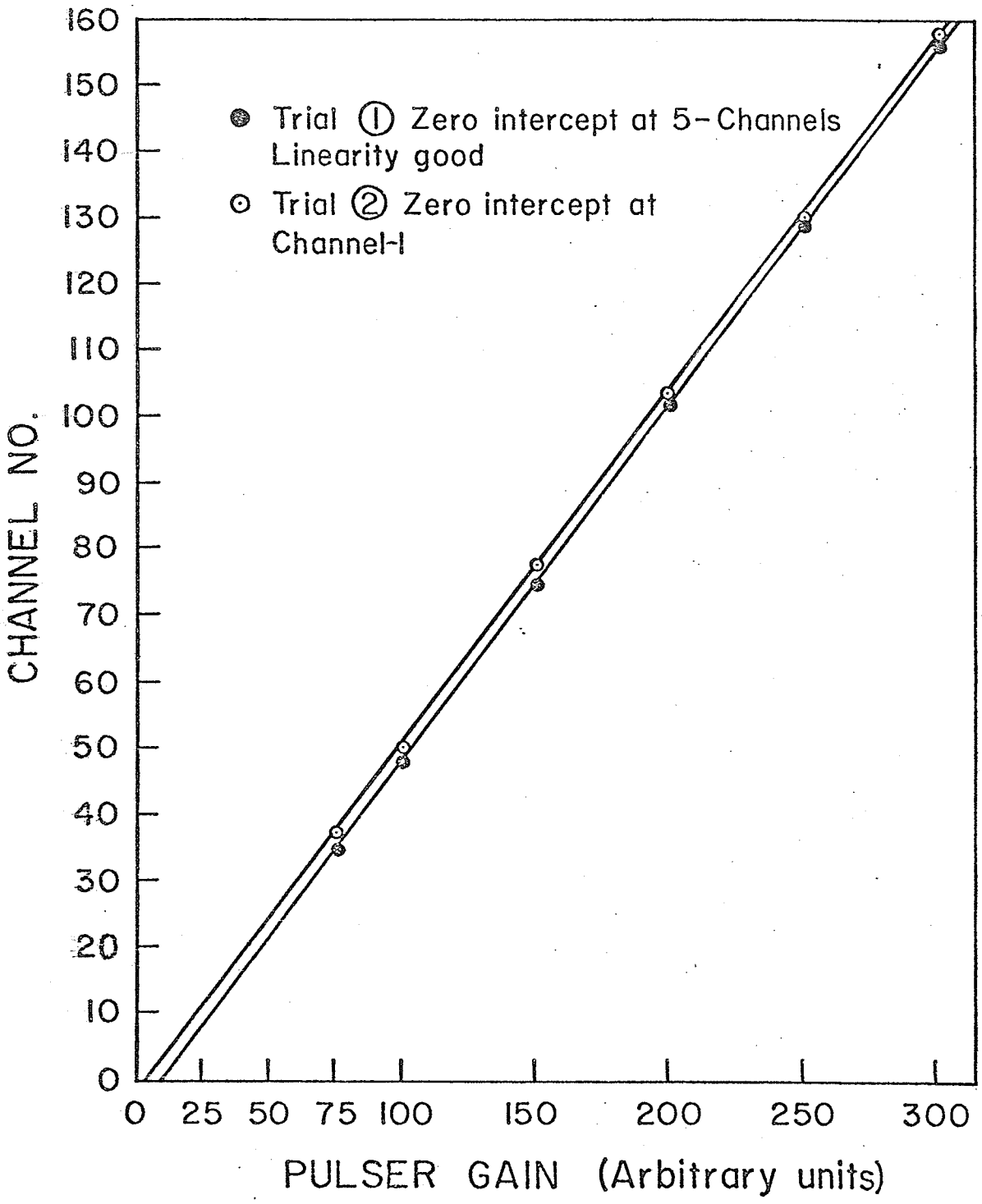
Trial ① Zero intercept at 5-Channels
Linearity good
Trial ② Zero intercept at
Channel-I
CHANNEL NO.
0
10
20
30
40
50
60
70
80
90
100
110
120
130
140
150
160
0 25 50 75 100 150 200 250 300
PULSER GAIN (Arbitrary units)

Fig. 2-6

The thresholds on the delta E TSCA 's were carefully adjusted so that none of the alpha particles were eliminated but that the faster protons which left very little energy in the delta E detector were rejected. Although the on-line computer could distinguish them from alpha particles this step greatly reduced the computer dead time. The E detectors TSCA 's threshold was set as low as possible so that none of the alpha particles would be unnecessarily filtered out.

The Camac ADC had a slightly higher gain than the Northern ADC so the data measured on the right detector system had a higher gain than that measured on the left. This was left to be accounted for during the data analysis.

The On-Line Computer

The PDP-15 computer was used to create two-dimensional displays (scatter plots) which plotted delta E versus E total for both left and right detector systems. Figure 2-7 shows a typical example. The different energy loss characteristics of the particles clearly separates the particles into narrow bands. Energy loss per unit path length increases with nucleon number and with the square of the nuclear charge.

A set of loci was drawn around the alpha particles as shown by the dashed lines on Figure 2.7 Another set of loci was drawn around the ^{3}He particles. A computer program was used to log the data on magnetic tape and to create energy spectra where only the events which were between the loci were plotted. Figure 2-8 shows a spectrum from all particles. Figure 2-9 shows only the alpha particles and Figure 2-10 shows only the ^{3}He particles for a typical run.

As can be seen by Figure 2-9, the low energy alpha particles are not seen in this type of measurement. This is because the alpha particles with

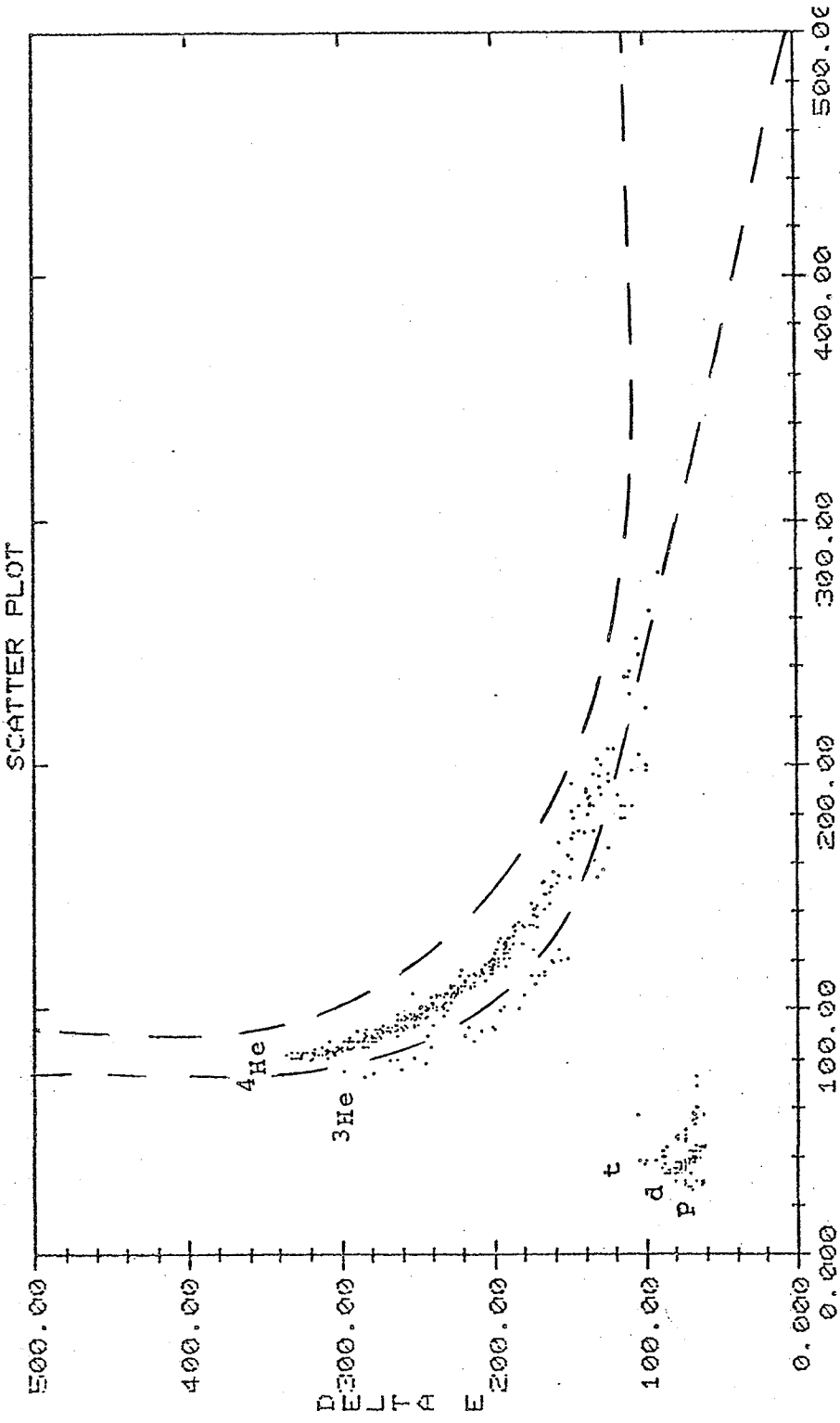
SCATTER PLOT
DELTA E
TOTAL ENERGY
500.00
400.00
300.00
200.00
100.00
0.000
0.000
100.00
200.00
300.00
400.00
500.00
4He
3He
t
d
p
BOTH ENERGY SCALES ARE IN ARBITRARY UNITS

Fig. 2-7

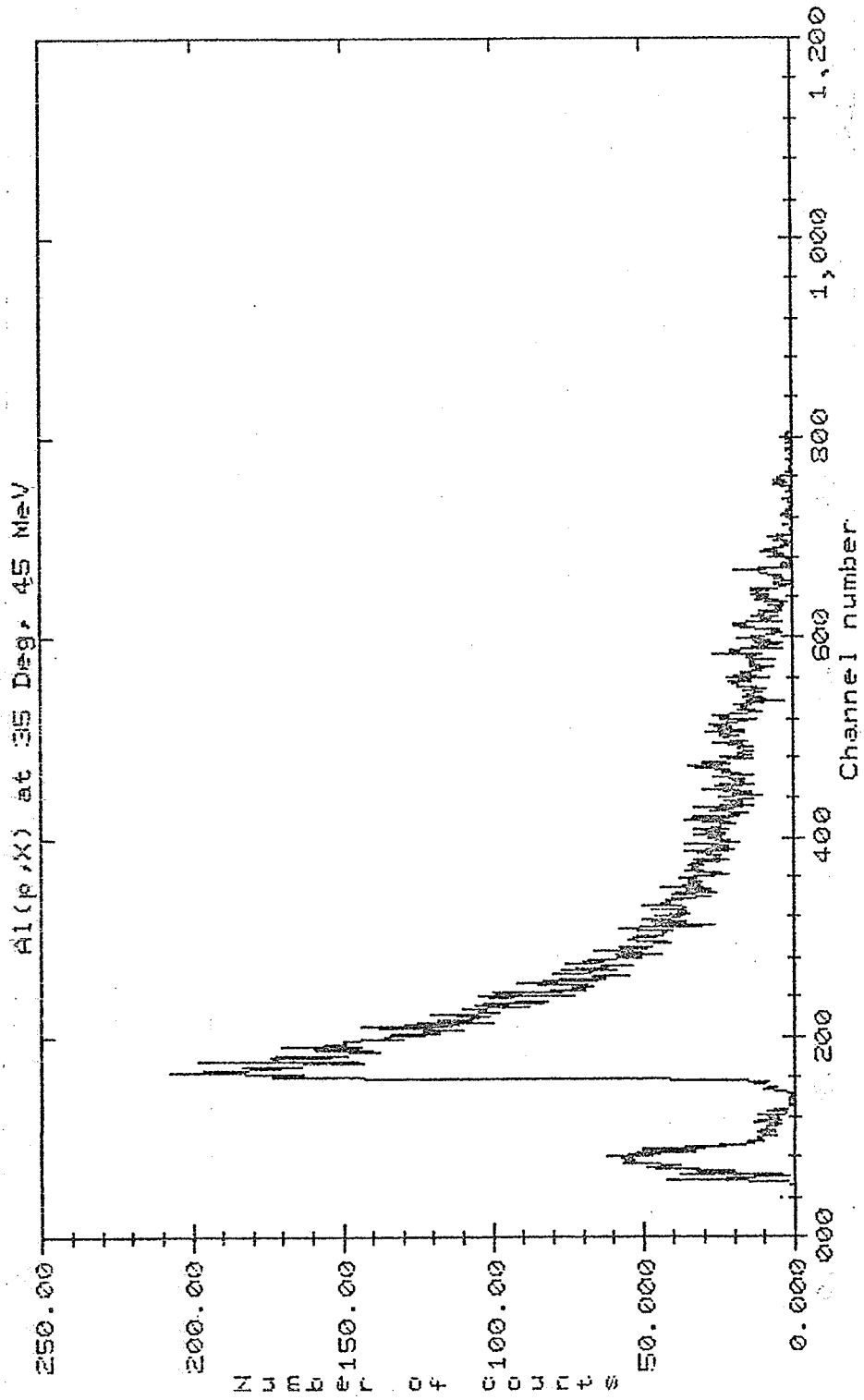
Al(p,X) at 35 Deg, 45 MeV
Number of counts
Channel number
250.00
200.00
150.00
100.00
50.000
0.0000
000
200
400
600
800
1,000
1,200

Fig. 2-8

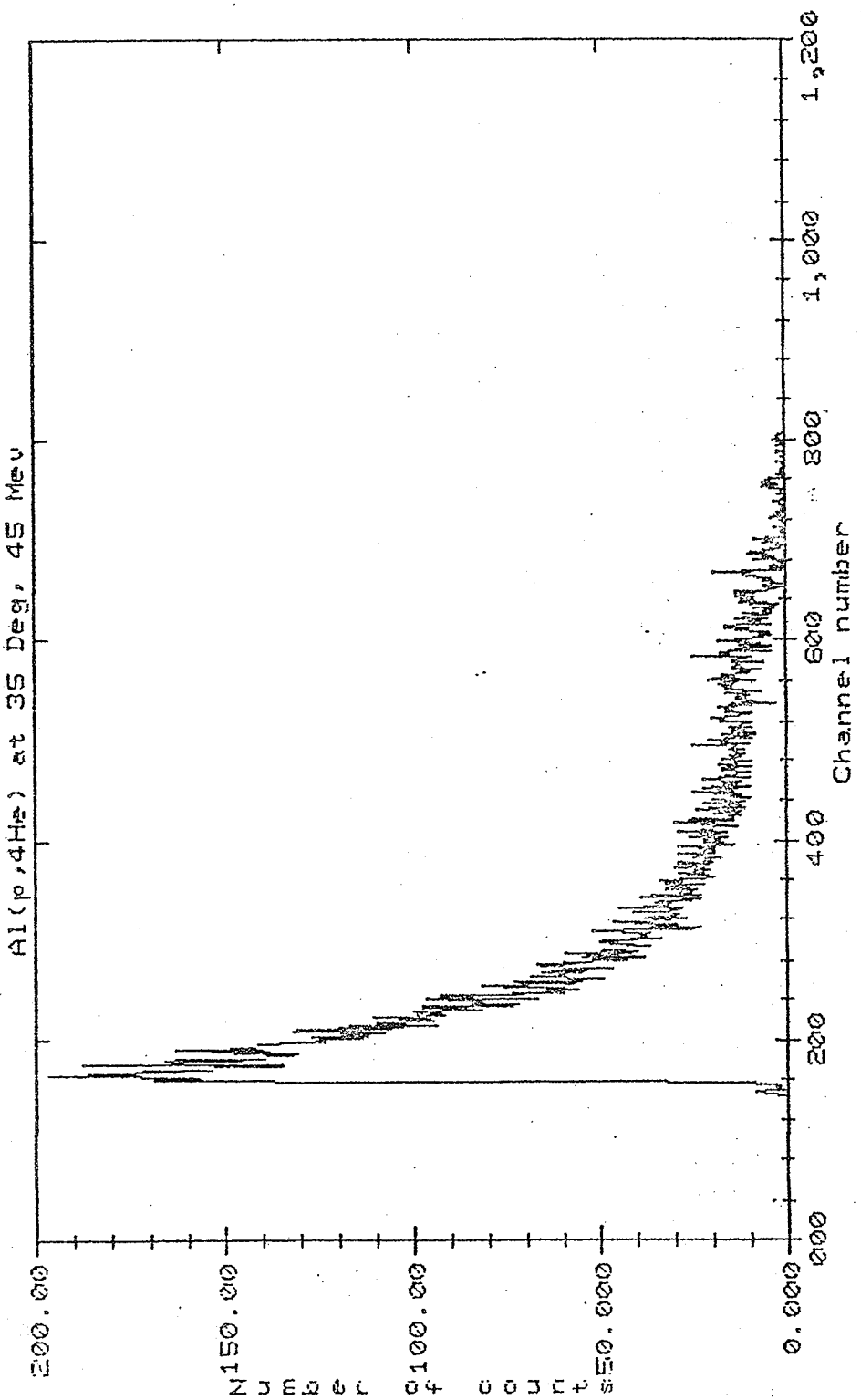
Al(p,4He) at 35 Deg, 45 Mev
Number of counts
200.00
150.00
100.00
50.000
0.000
000
200
400
600
800
1,000
1,200
Channel number

Fig. 2-9

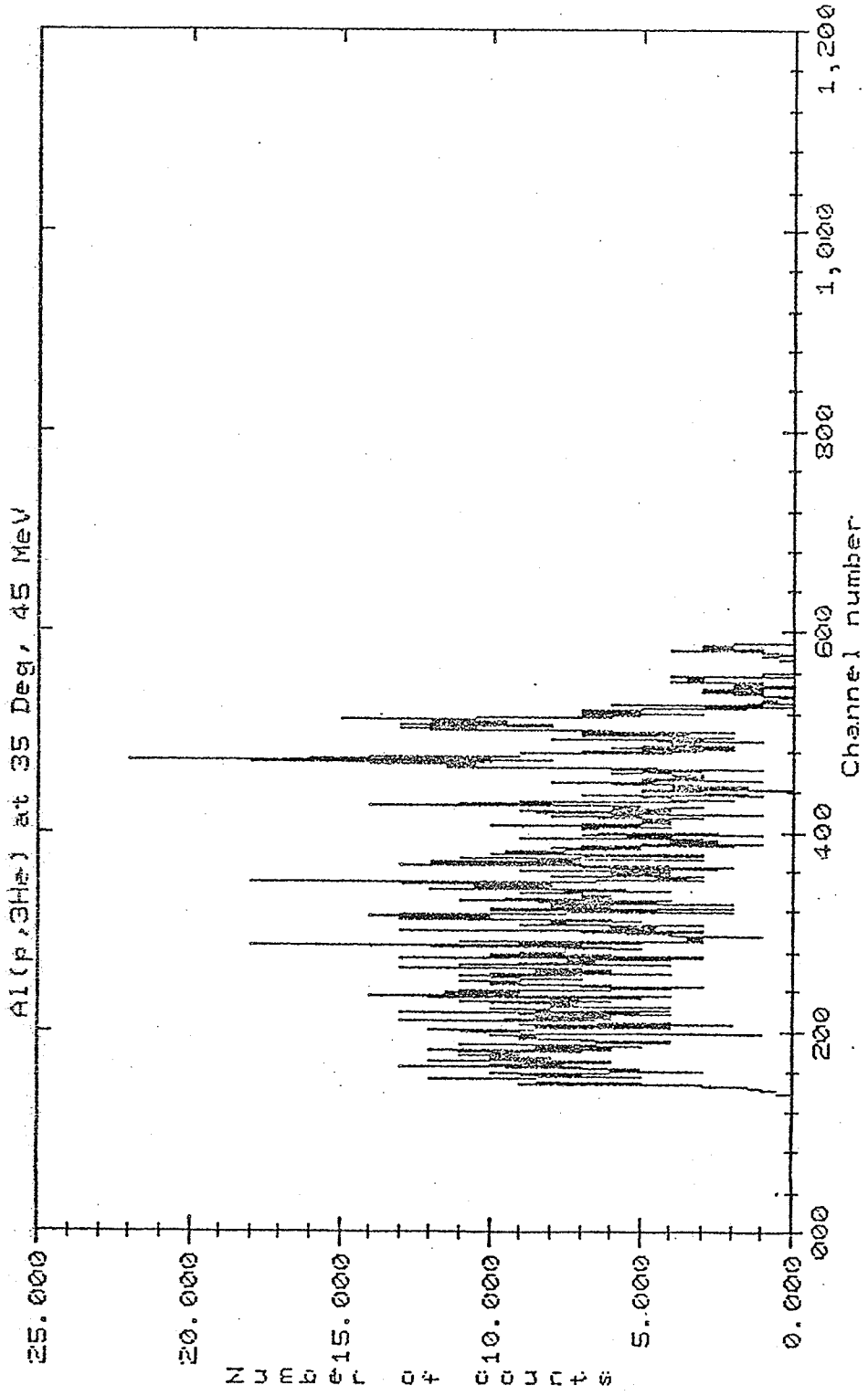
Al(p,3He) at 35 Deg, 45 MeV
Number of counts
Channel number
25.000
20.000
15.000
10.000
5.000
0.000
000
200
400
600
800
1,000
1,200

Fig. 2-10

less than 8 MeV, do not make it through the delta E detector into the E detector and thus the coincidence requirement rules them out. Because these spectra are cut off below 8 MeV it is difficult to extrapolate them to zero energy. Therefore the coincidence requirements were removed and spectra were taken at approximately seven different angles. Figure 2-11 shows how the loci were drawn for these measurements. Clearly the resulting spectrum on Figure 2-12 now contains alpha and ^{3}He particles although all protons, deuterons and tritons have been eliminated. However the ^{3}He particles make up less than ten percent of the total counts at high energy and a correspondingly low fraction at low energy. Thus these data show the shape of the low energy alpha spectrum. These measurements give information on the alpha particle spectrum between 3 and 8 MeV and thus make it easier to extrapolate the cross sections to zero energy.

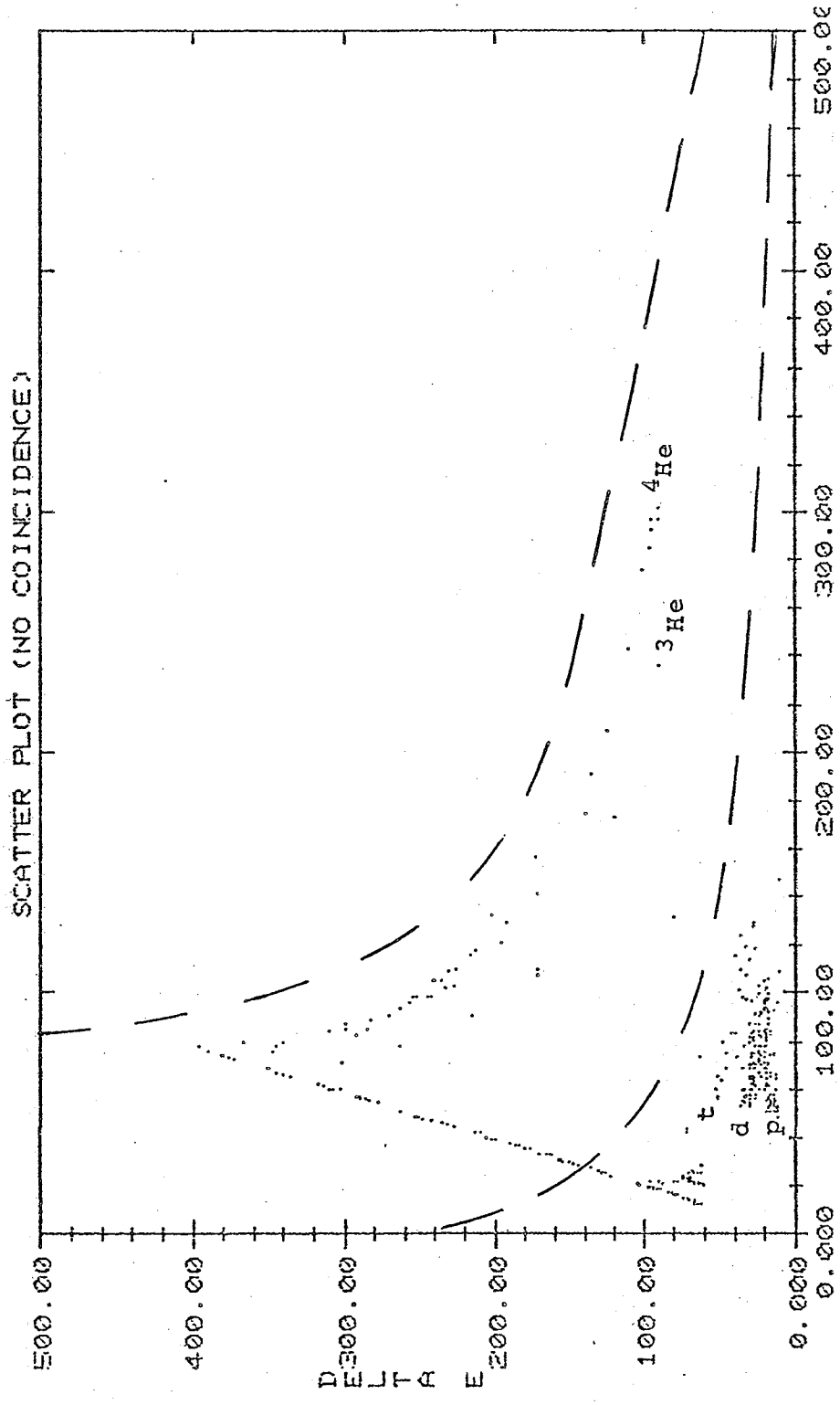

BOTH ENERGY SCALES ARE IN ARBITRARY UNITS

Fig. 2-11

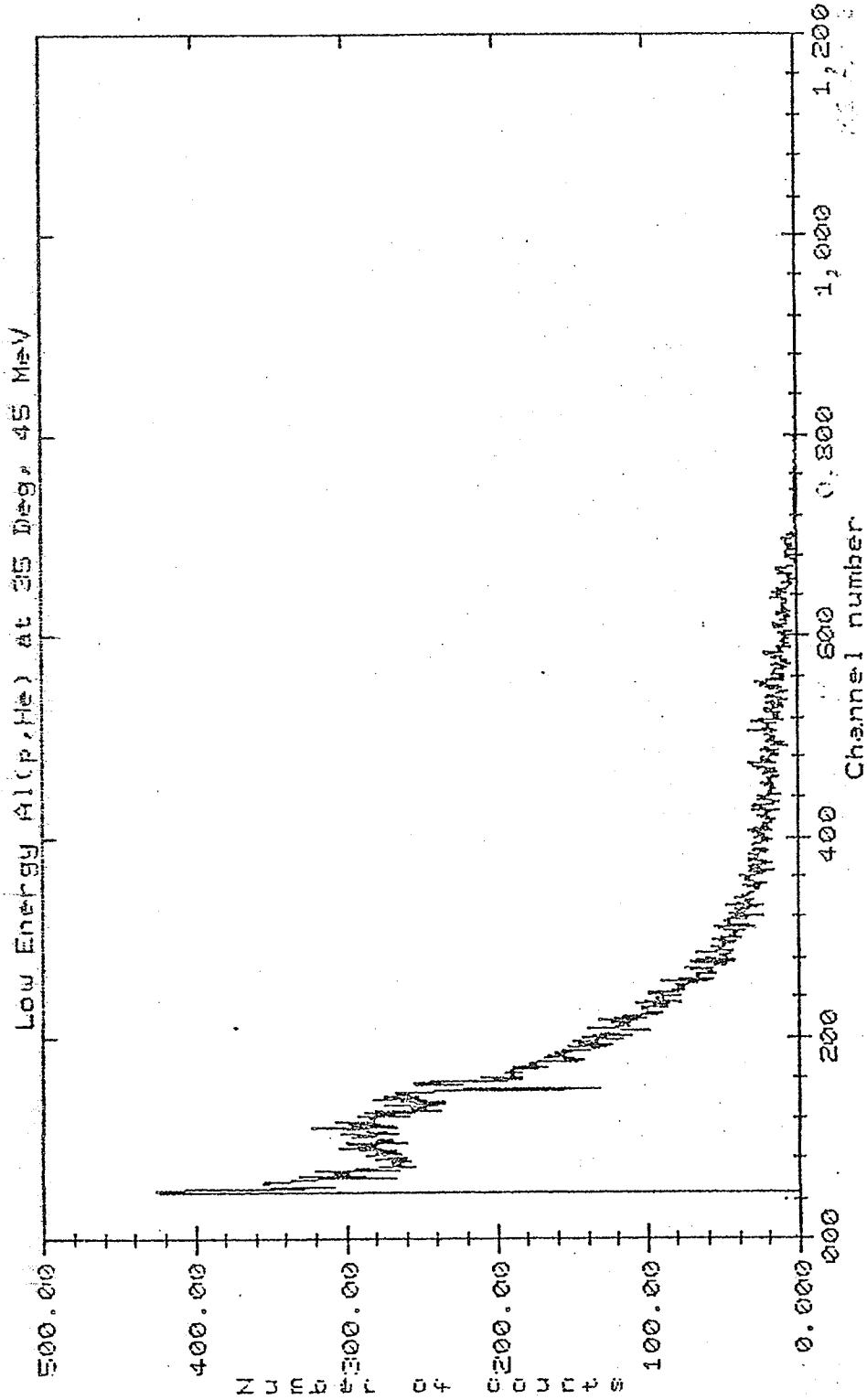
Low Energy Al(p,He) at 35 Deg, 45 MeV
Number of Counts
500.000
400.000
300.000
200.000
100.000
0.000
000
200
400
800
1,000
1,200
Channel number

Fig. 2-12

CHAPTER III

DATA ANALYSIS

Dead Layer Corrections

Two factors caused distortions in the low energy region of the spectra.

After the loci were drawn with the detectors set at medium angles it was noticed that when the detectors were moved to forward angles some of the triton events were allowed into the low energy portion of the helium data. This appears as the peak located at about channel 50 in Figure 3-1 which is a typical example.

Figure 3-1 also shows a drop in the number of counts at channel 160 and a slight excess on either side. This distortion was caused by dead layers between the detectors and by the E timing single channel analyser's threshold. Even though the E threshold was turned down as low as possible some events were still rejected.

In order to correct for these distortions a fifth degree polynomial function was fitted to the data, excluding the distorted regions. A typical fit is shown by the solid line in Figure 3-1. Although the polynomial shown goes through the origin, no knowledge of the spectra below the lowest energy measured data was used in any further analysis.

Low Energy Addition to the Spectra

The next step in the data analysis was to add the low energy portion of the spectra (3 to 8 MeV) onto the high energy portion of the spectra. This could not be done directly because the low energy portion contained ^{3}He particles as well as alpha particles and thus had a slightly larger number of counts than it should. Two methods were developed to correct

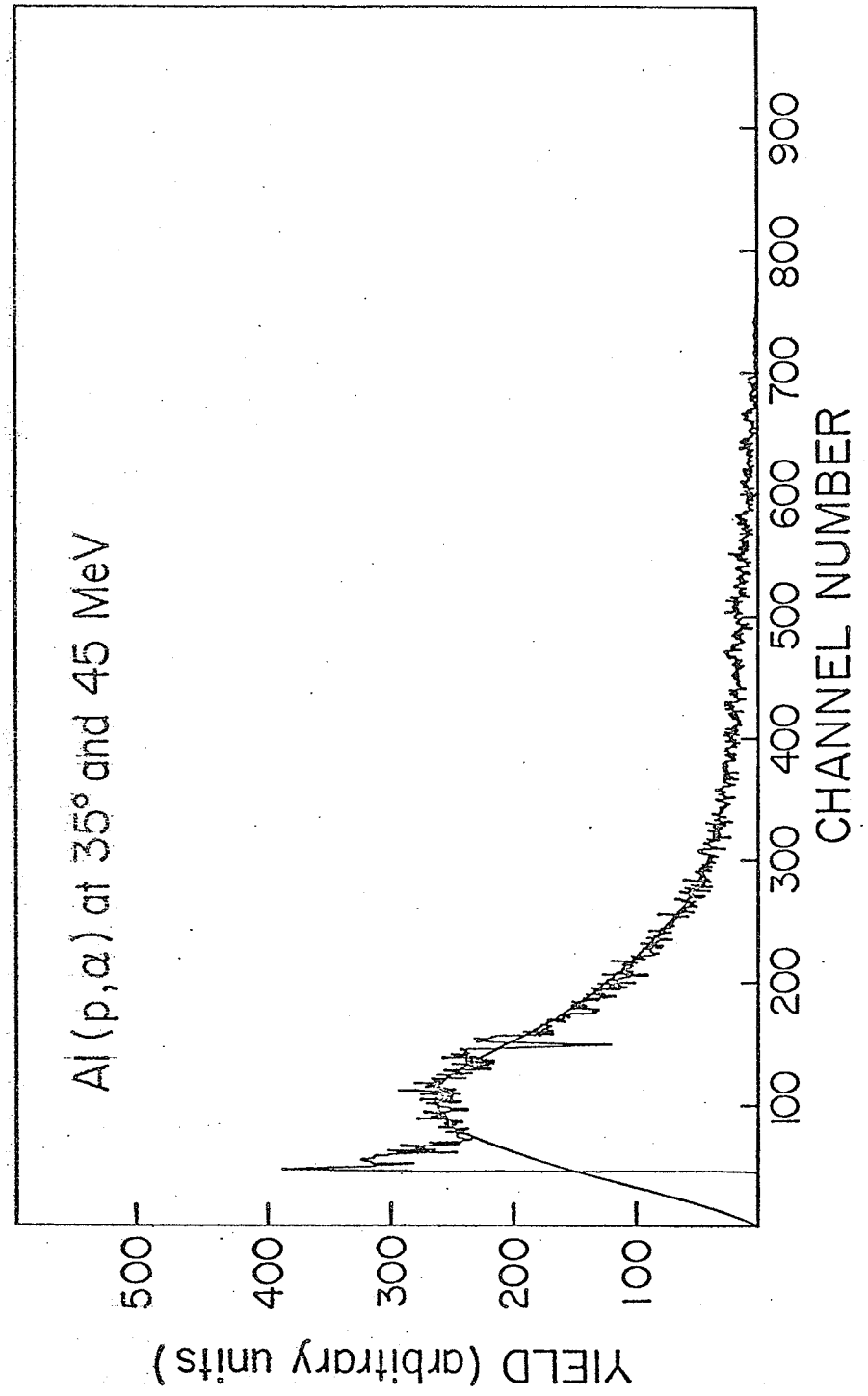
Al (p,α) at 35° and 45 MeV
YIELD (arbitrary units)
500
400
300
200
100
100
200
300
400
500
600
700
800
900
CHANNEL NUMBER

Fig. 3-1

for this. The first was to multiply the number of counts in each channel of the low energy data by a common correction factor (about 0.92) such that the low energy data joined smoothly onto the high energy data. The second method was to assume that the percentage of ^{3}He particles in the low energy data was the same as that in the lowest part of the high energy data. This percentage was then subtracted. Both these methods gave very similar results with differences of less than one percent in all spectra tested. The first method was chosen and used for the data analysis because of its easier implementation.

Thick Target Correction Formulae

As mentioned in chapter 2 the aluminum target was $2.28 \pm .05$ mg/cm^2 thick and the silicon target was $9.32 \pm .02$ mg/cm^2 thick. The thickness of the target presented a problem because particles produced in the target had to travel through part of the target before they got to the detectors. In doing so, they lost energy due to ionization. The slowest particles were completely stopped and thus lost from the measured spectra. It is important to correct for this energy shift and particle loss in order to get the true alpha particle spectra as would be produced in an infinitestimal target. For our silicon measurements at 50 degrees the alpha particles produced on the side of the target furthest from the detectors had to travel through 14.5 mg/cm^2 of silicon. This was enough to stop a 10 MeV. alpha particle so it was imperative to make this correction.

Two methods of correcting for thick target effects have been described in the literature. One was an algebraic solution using the range-energy relation and was presented by Comiso et al.[9] The other was a matrix solution using the stopping power-energy relation and was presented by Johnson et al.[10] If the method of Johnson et al. was used for

our 1024 channel spectra then the matrices would have been huge and the computing time would have been excessively long. Comiso et al.'s method was much simpler but was valid only for cases where none of the particles produced in the target had ranges greater than the total target thickness. This method therefore was not applicable to our experiment where many of the particles had energies considerably greater than that which the target could stop. The following is a derivation of a thick target correction formula. It follows the method of Comiso et al. closely.

The measured yield of alpha particles is given by

$$Y = nN \Delta\Omega \frac{d\sigma}{d\Omega}$$

where $\frac{d\sigma}{d\Omega}$ is the differential cross section in cm^2

$\Delta\Omega$ is the solid angle in steradians. The assumption is made that the beam spot size and target thickness are small compared with the distance between the target and the detectors so that any variations in angle caused by the location of the alpha particle production are negligible.

n is the total number of incident particles.

N is the total number of target nuclei in number of atoms/cm^2.

$$N = \frac{tpA}{u}$$

where:

t = target thickness in cm

p = target density in g/cm^3

A = Avogadros number in number of atoms/mole

u = atomic weight in g/mole

Now Y is properly a function of both angle and energy, or

$$y(\theta,E) = nN\Delta\Omega\Delta E \frac{d\sigma}{d\Omega dE},$$

$$\frac{dY(\theta,E)}{dE} = nN\Delta\Omega \frac{d\sigma}{d\Omega dE}$$

But properly $\frac{d\sigma}{d\Omega dE}$ refers to a threefold differential cross section (in cm^2/MeV-steradian) for an infinitesimal target. Thus assuming σ does not change over the target thickness with incident energy:

$$\frac{d}{dx}\frac{dY(\theta,E)}{dE} = \frac{nN}{L}\Delta\Omega \frac{d\sigma}{d\Omega dE}$$

x is the distance the particle travels through the target and $0 \leq x \leq L$ where L = target thickness in cm/cosθ and is the effective thickness for outgoing alphas.

Now let Em and Rm be the measured energy and range respectively and Ep and Rp be the energy and range that the particle was produced with.

$$\frac{d}{dx}\frac{dY(\theta,Ep)}{dEp} = \frac{nN}{L}\Delta\Omega \frac{d\sigma}{d\Omega dEp}$$

let $P(Ep) = \Delta\Omega \frac{d\sigma}{d\Omega dEp}$

$$\frac{d}{dx}\frac{dY(\theta,Ep)}{dEp} = \frac{d}{dx}\frac{dY(\theta,Em)}{dEp} = \frac{nN}{L}P(Ep), \text{ since Em = function of Ep}$$

Now integrating over the distance x one obtains:

$$dY(\theta,Em) = \frac{nN}{L}\int_0^\infty P(Ep)\,dEp\,dx$$

$$\frac{\partial(x,Ep)}{\partial(x,Em)} = \frac{\partial Ep}{\partial Em} = \frac{\partial Ep}{\partial Rm}\,x\,\frac{\partial Em}{\partial Rm}\,x$$

Therefore $\frac{dY(\theta,Em)}{dEm} = \frac{nN}{L}\frac{\partial Rm}{\partial Em}\int_0^\infty P(Ep)\frac{\partial Ep}{\partial Rm}\,dx$

$\frac{dY(\theta,Em)}{dEm} = V(Em)$ which is the measured yield per unit of energy (MeV)

Now $R(Ep) = Rm + x$

$$Ep = E(Rm + x)$$

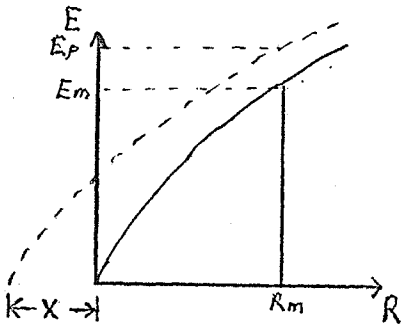

$$\left(\frac{\partial\ Ep}{\partial\ Rm}\right)_X dx = \frac{\partial\ Ep}{\partial\ Rp}\ \frac{\partial\ Rp}{\partial\ Rm}\ dx = dEp$$

$$V\ (Em) = \frac{nN}{L}\ \frac{\partial\ Rm}{\partial\ Em}\ \int_{Em}^{Emax} P(Ep)\ dEp$$

where $Emax = E\ (Rm + L)$

Differentiating one obtains:

$$V''(Em) = \frac{nN}{L}\left(\frac{d^2 Rm}{dEm^2}\right) \int_{Em}^{Emax} P\ (Ep)\ dEp$$

$$+ \frac{nN}{L}\left(\frac{dRm}{dEm}\right)^2 \Big/ \frac{dRmax}{dEmax}\ P\ (Emax)$$

$$- \frac{nN}{L}\ \frac{dRm}{dEm}\ P\ (Em)$$

Now substituting in to eliminate the integral.

$$V''(Em) = \frac{d^2 Rm}{dEm^2} \Big/ \frac{dRm}{dEm}\ V\ (Em)$$

$$+ \frac{nN}{L}\left(\frac{dRm}{dEm}\right)^2 \Big/ \left(\frac{dRmax}{dEmax}\right) P\ (Emax)$$

$$- \frac{nN}{L}\left(\frac{dRm}{dEm}\right) P\ (Em)$$

Rearranging: $$\frac{nN}{L} P\ (Em) = \frac{d^2 Rm}{dEm^2} \Big/ \left(\frac{dRm}{dEm}\right)^2 V\ (Em) - 1 \Big/ \left(\frac{dRm}{dEm}\right) V'\ (Em)$$

$$+ \frac{nN}{L}\left(\frac{dRm}{dEm}\right) \Big/ \left(\frac{dRmax}{dEmax}\right) P\ (Emax)$$

$\frac{d\sigma}{dE} = P\ (Em)$ is the produced yield per unit energy (MeV)

The thick target correction formula can be written as:

$$\frac{d\sigma}{dE} = \frac{L}{nN}\left[\frac{\left(\frac{d^2 R}{dE^2}\right)}{\left(\frac{dR}{dE}\right)^2}\ \frac{d\ Y\ (\theta,\ E)}{dE} - \frac{\frac{d^2\ Y(\theta,\ E)}{dE^2}}{\left(\frac{dR}{dE}\right)}\right]$$

$$+ \frac{\left(\frac{dR}{dE}\right)}{\left(\frac{dR}{dE}\right)_{E\ =\ E\ (R+L)}}\left(\frac{d\sigma}{dE}\right)_{E\ =\ E\ (R+L)}$$

We need a continuous energy spectrum.

This equation may at first look insolvable but by starting at channel 1024 where $\left(\frac{d\sigma}{dE}\right)_{E = E\ (R+L)}$ equals zero and then working back one can numerically calculate the complete spectrum of produced particles.

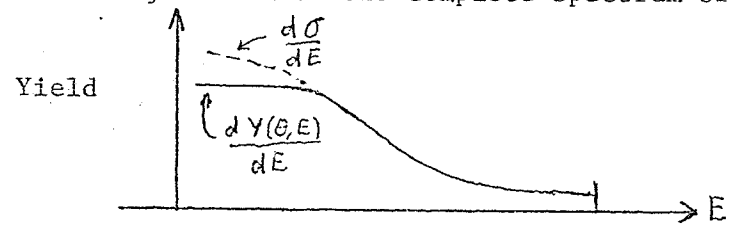

Notice that if one considers targets which are thick enough that none of the produced particles is energetic enough to pass through the complete target then $\left(\frac{d\sigma}{dE}\right)_{E = (R+L)}$ is always equal to zero and our thick target correction formula reduces to

$$\left(\frac{d\sigma}{dE}\right) = \frac{L}{nN}\left[\frac{\left(\frac{d^2R}{dE^2}\right)}{\left(\frac{dR}{dE}\right)^2}\ \frac{dY(\theta, E)}{dE} - \frac{\frac{d^2Y(\theta, E)}{dE^2}}{\left(\frac{dR}{dE}\right)}\right]$$

as derived by Comiso et al.[9]

In order to do the thick target correction one must fit the analytical expressions to R (E) and $\frac{dY(\theta, E)}{dE}$ as functions of energy. Then these analytical expressions must be differentiated to produce $\left(\frac{dR}{dE}\right)$; $\left(\frac{d^2R}{dE^2}\right)$; $\frac{d^2Y(\theta, E)}{dE^2}$ which are terms in the correction formulas.

One aspect not taken into consideration is range straggling. Comiso et al[9] tested for the effects of this and found them to be small. It is assumed that the straggling in range between particles of close energy will cancel in such a way that the effects in smooth spectra such as the ones under consideration would not be noticeable.

Range-Energy Relationships

In order to calculate the thick target correction a very accurate range-energy relation is needed. The initial attempt to obtain this relationship was to use the formula: $R = 0.295 \cdot E^{1.73}$ which was given by Goulding et al.[11] This formula was presented as being reliable between 10 and 100. MeV. Comparing the predictions with the range of alpha particles in silicon from Marion and Young[12] shows the predictions to be poor at lower energies. Even when the two constants were adjusted slightly to give a better fit, the calculations gave still poor representation below ten MeV.

Thus several polynomial fits to the range-energy data for alpha particles in aluminum were tried. The data table used was the one supplied by Northcliffe and Schilling.[13] Comiso et al[9] reported it to be the best at low energy. It covered the needed energy range rather well.

Table 3-1 shows the best fit to the data that could be obtained. The computer program used to obtain this fit is contained in Appendix I. The error is 0.59×10^{-4} as calculated by

$$\text{error} = \frac{\sum_{i=1}^{N} (Y(i) - Z(i))^2}{N - D - 1}$$

where $Y(i)$ = the data table range for energy point number i.

$Z(i)$ = the calculated range at energy point number i.

N = the number of data points

D = the degree of the polynomial

Other polynomial fit programs which were tried could not do as good a job.

The co-efficients from Table 3-1 correspond to a seventh degree polynomial. The polynomial was then differentiated to produce the needed $\partial R/\partial E$ and $\partial^2 R/\partial E^2$ energy dependancies. These relationships with energy were the ones used in the thick target correction.

TABLE 3-1

Energy	Data Tables (13) Range in mg/cm^2	Calculated Range in mg/cm^2
0.5003	0.5740	0.5857
0.6404	0.6800	0.6821
0.8005	0.8020	0.7981
1.0007	1.1910	1.1825
1.6010	1.4750	1.4688
2.0013	1.8600	1.8598
2.4016	2.2830	2.2873
2.8018	2.7450	2.7505
3.2021	3.2440	3.2490
3.6023	3.7790	3.7823
4.0026	4.3490	4.3500
5.0033	5.9200	5.9169
6.4042	8.4600	8.4552
8.0052	11.8350	11.8325
10.0070	16.7420	16.7452
12.8080	24.8570	24.8488
16.0100	35.8380	35.8368
20.0130	52.0110	52.0098
24.0160	70.7870	70.7889
28.0180	92.0630	92.0616
32.0210	115.7520	115.7527
36.0230	141.7630	141.7828
40.0260	170.0920	170.0920

A 1 = 0.28031047D+00
A 2 = 0.54906892D+00
A 3 = 0.12366895D+00
A 4 = -.19611173D-02
A 5 = 0.71534988D-04
A 6 = -.19288997D-05
A 7 = 0.29340044D-07
A 8 = -.18608327D-09

Twelve data points with energies less than 0.5 MeV are found in the Northcliff and Schilling data tables.[13] These points were ignored in order to obtain a better fit for the remaining data. This was judged to be acceptable because we had no data below 3 MeV due to triton contamination. The spectra were extrapolated between zero and 3 MeV as will be explained later in this chapter.

The correction term in the thick target calculations requires the calculation of Emax where Emax is the energy of a particle with a range equal to the range of E_m plus L, the effective target thickness. Thus it is also necessary to obtain a relationship for the energy in terms of the range. The inverse function of the polynomial given in Table 3-1 would be difficult to calculate. Therefore the program in Appendix I was used to fit the energy to the range data.[13] The best fit is shown in Table 3-2 and the error is now equal to 0.79×10^{-3} as calculated by the formula given previously.

The Measured Spectra

Both the measured spectra and their first derivatives with respect to energy were used in the thick target correction calculations. The measured spectra naturally contained a certain amount of random variation between the points due to statistical fluctuations. To eliminate the fluctuations smooth curves were produced by fitting polynomials to the data points. Figure 3-2 shows a typical example. These new curves were then used to calculate the derivative of the measured spectra by simply comparing neighbouring points. No attempt to fit the very high energy features was attempted because the errors in the slope would have been large. The very high end of the measured spectrum was instead added onto the thick target corrected spectrum. This will be illustrated later in this chapter. This produced spectra which were distorted in the very high

TABLE 3-2

Range in mg/cm^2	Energy from Data Tables (13) (MeV)	Calculated Energy (MeV)
0.1420	0.0500	0.0449
0.1660	0.0640	0.0662
0.1900	0.0801	0.0881
0.2180	0.1001	0.1143
0.2520	0.1281	0.1470
0.2880	0.1601	0.1827
0.3270	0.2001	0.2226
0.3650	0.2402	0.2625
0.4000	0.2802	0.3000
0.4330	0.3202	0.3361
0.4650	0.3602	0.3717
0.4970	0.4003	0.4078
0.5740	0.5003	0.4965
0.6800	0.6404	0.6221
0.8020	0.8005	0.7699
0.9590	1.0007	0.9628
1.1910	1.2808	1.2472
1.4750	1.6010	1.5850
1.8600	2.0013	2.0116
2.2830	2.4016	2.4305
2.7450	2.8018	2.8314
3.2440	3.2021	3.2128
3.7790	3.6023	3.5853
4.3490	4.0026	3.9659
5.9200	5.0033	5.0226
8.4600	6.4042	6.3992
11.8350	8.0052	8.0049
16.7420	10.0070	10.0087
24.8570	12.8080	12.8197

A 1 = -.67805910D-01
A 2 = 0.70569696D+00
A 3 = 0.67189260D+00
A 4 = -.37791931D+00
A 5 = 0.92570545D-01
A 6 = -.11951416D-01
A 7 = 0.83186985D-03
A 8 = -.29182169D-04
A 9 = 0.40028288D-06

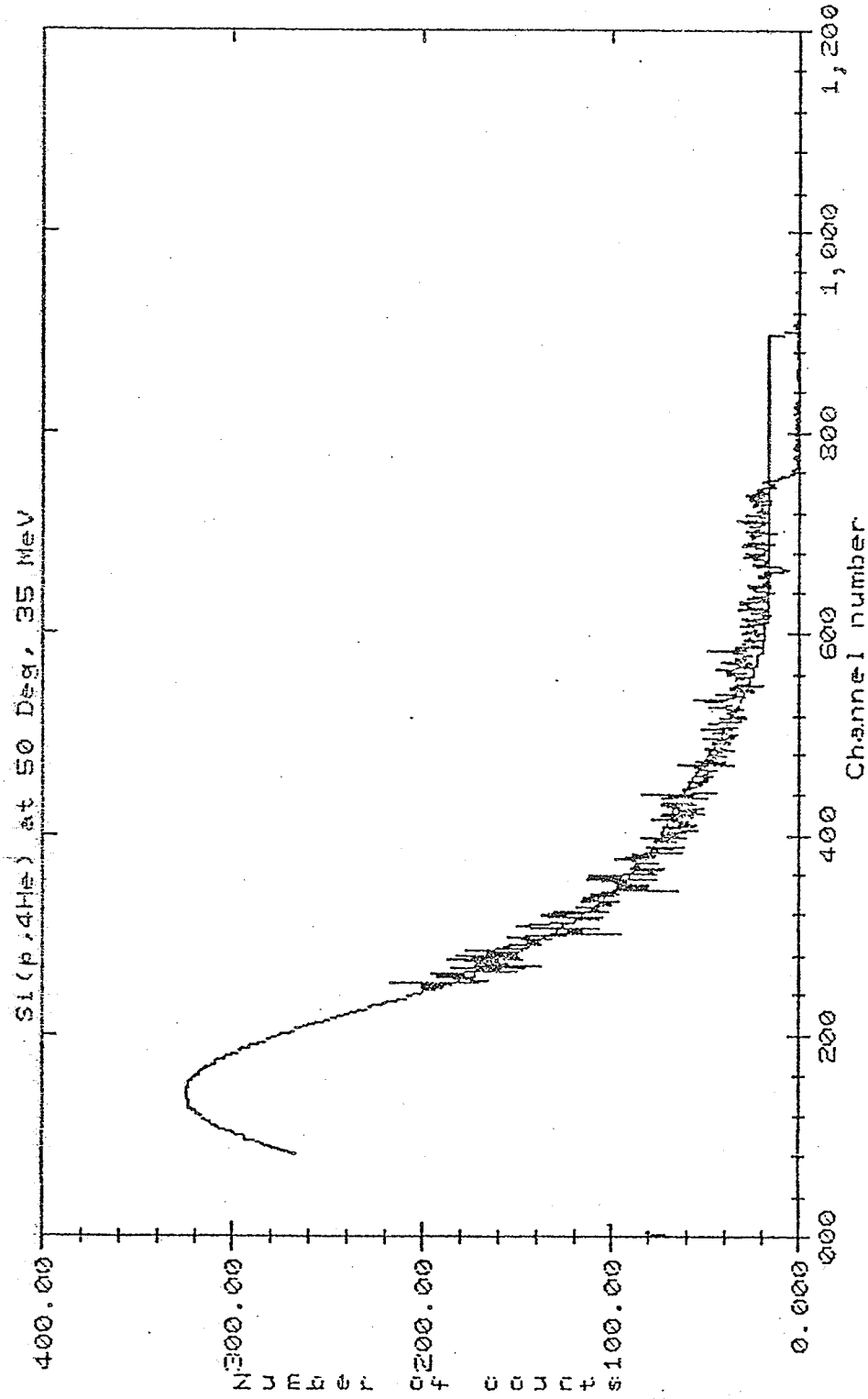
Si(p,4He) at 50 Deg, 35 MeV
Number of counts
400.000
300.00
200.00
100.00
0.000
000
200
400
600
800
1,000
1,200
Channel number

Fig. 3-2

energy region from the produced spectra. Although some of the particles were slowed down (never by more than 2 MeV) by the target, none were stopped so the final spectra contained the right number of counts.

The final factor needed for the computer calculations is the ratio between energy and channel number. This conversion factor was obtained by comparing the energy of the highest energy aluminum peak with a relativistic two body kinematics calculation for that energy. Table 3-3 shows the 45 MeV results. This gave the channel number to MeV conversions of Table 3-4.

TABLE 3-3

MEASURED GAINS AT 45 MeV

Spectrum	Left Channel	Right Channel	Energy (MeV)	Left Conversion Factor MeV/channel	Right Conversion Factor MeV/channel
Al at 35°	788	802	43.52	.05522	.05426
Al at 90°	691	704	38.24	.05535	.05433

TABLE 3-4

CONVERSION FACTORS USED IN THE CALCULATIONS

	Left (MeV/Channel)	Right (MeV/Channel)
45.0 MeV	.05529	.05429
35.0 MeV	.03744	.03609

Thick Target Correction Computer Code

The computer code for the thick target correction is contained in Appendix 2. Pages 67 to 71 contain the main data handling program. Its functions are:

1) input of spectra from magnetic tape and display on a screen
2) change of the scale of a spectrum by multiplying the number of counts in each channel by a common factor
3) typing out of number of counts versus channel number
4) fitting of a polynomial up to 10th order through whatever channels were selected and generation of a new spectrum using the calculated polynomial
5) addition of part of one spectrum onto another spectrum
6) storing and outputting of files which were created.

The polynomial fit was important in that it could correct for the dead layer distortions mentioned earlier by fitting a curve through the undistorted points on each side. The actual subroutine which does the polynomial fitting is shown in page 73 which is in Appendix 2.

This program could also do thick target corrections by calling the subroutine on page 72 which is in Appendix 2. The program starts at the highest energy point and calculates the new spectrum channel by channel by using the thick target correction formula which was presented earlier. The coefficients for the range-energy relationships were used to calculate many of the terms. The original measured spectrum was used for the measured spectrum term but for its first derivative the smooth spectrum generated by the polynomial fit, was used.

Pages 74 and 76 of Appendix 2 show the smoothing routines which could accurately smooth the data by using cubic splines. A faster but less accurate smoothing routine is located in the main program. Several other small subroutines were necessary to run the program but these are not shown.

As mentioned earlier no attempt was made to fit the slope of the measured spectrum to the very high energy features. Thus the original

high energy end of the measured spectrum was added onto the corrected spectrum. Figures 3-3 and 3-4 illustrate how this was done for one spectrum. The portion of the measured spectrum above channel number 400 was added onto the thick target corrected spectrum.

Figure 3-4 also shows how the corrected spectrum was extrapolated from the 3 MeV cut off energy down to zero yield at zero energy. From phase space arguments [15] one knows that the differential cross section varies as the square root of the energy at low energies. This information was used in selecting the shape of the extrapolated section of the spectrum.

Test of Thick Target Correction

In order to test the accuracy of the thick target correction we took the thick target corrected spectrum, simulated the passage of particles through a target, and then checked if the resulting spectrum was the same as the measured spectrum. Appendix 3 shows the subroutine used to simulate the target. The main program is not shown because it is very similar to the main program in Appendix 2. The subroutine uses the same polynomials for the energy range relationship as the thick target correction code used.

The subroutine took the number of counts in one channel of the corrected spectrum, assumed that 1/20th of that number were produced in the centre of each of 20 target slices, and then produced a new spectrum by calculating how much energy the particles in each location lost when travelling through the target to the detectors. Figures 3-5 to 3-7 show in turn a measured spectrum, a thick target corrected spectrum and then the spectrum produced by simulating a target being added to the corrected spectrum. In general, the final spectrum agreed very closely with the

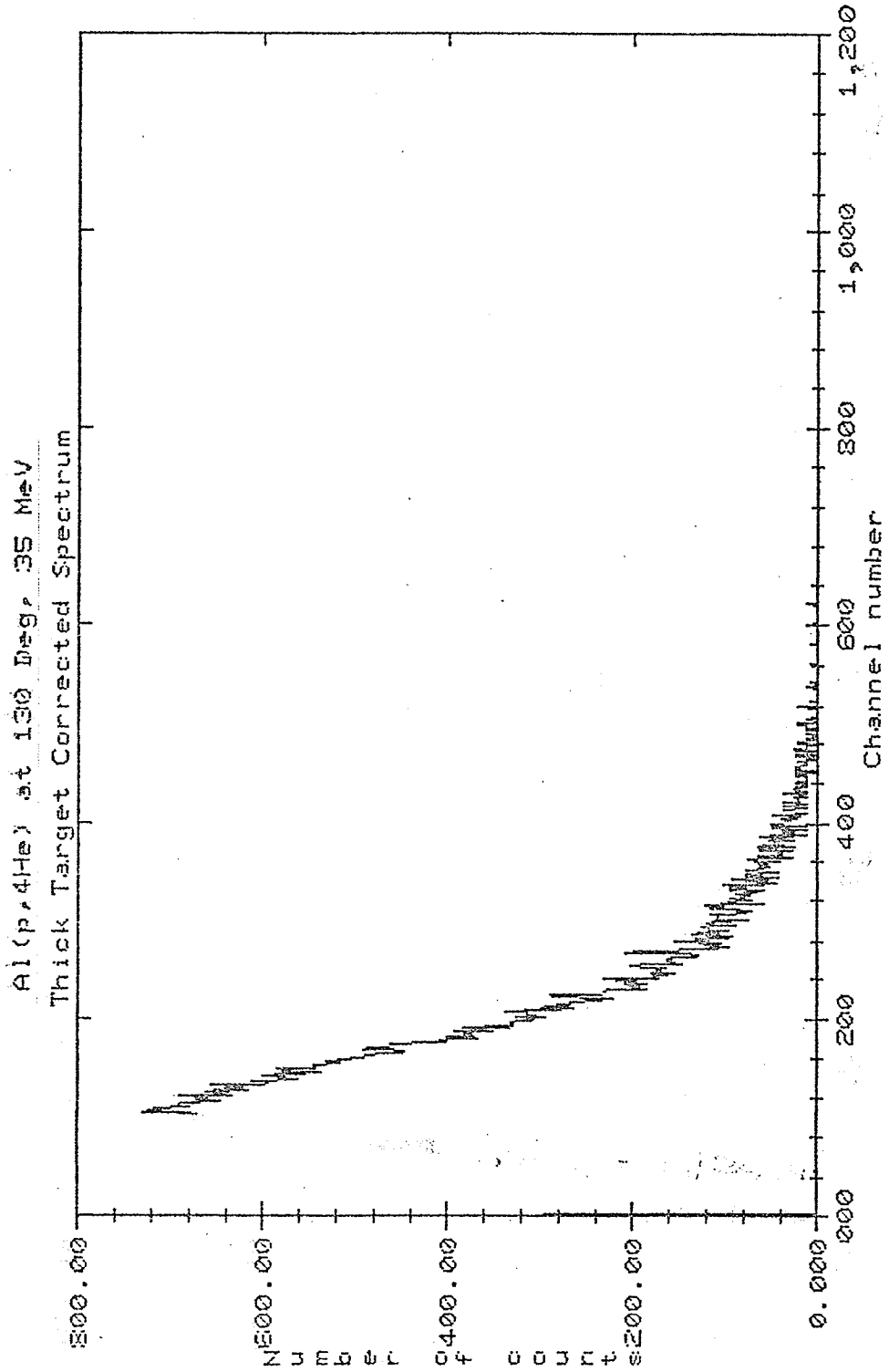
Al(p,4He) at 130 Deg, 35 MeV
Thick Target Corrected Spectrum
Number of Counts
800.00
600.00
400.00
200.00
0.000
200
400
600
800
1,000
1,200
Channel number

Fig. 3-3

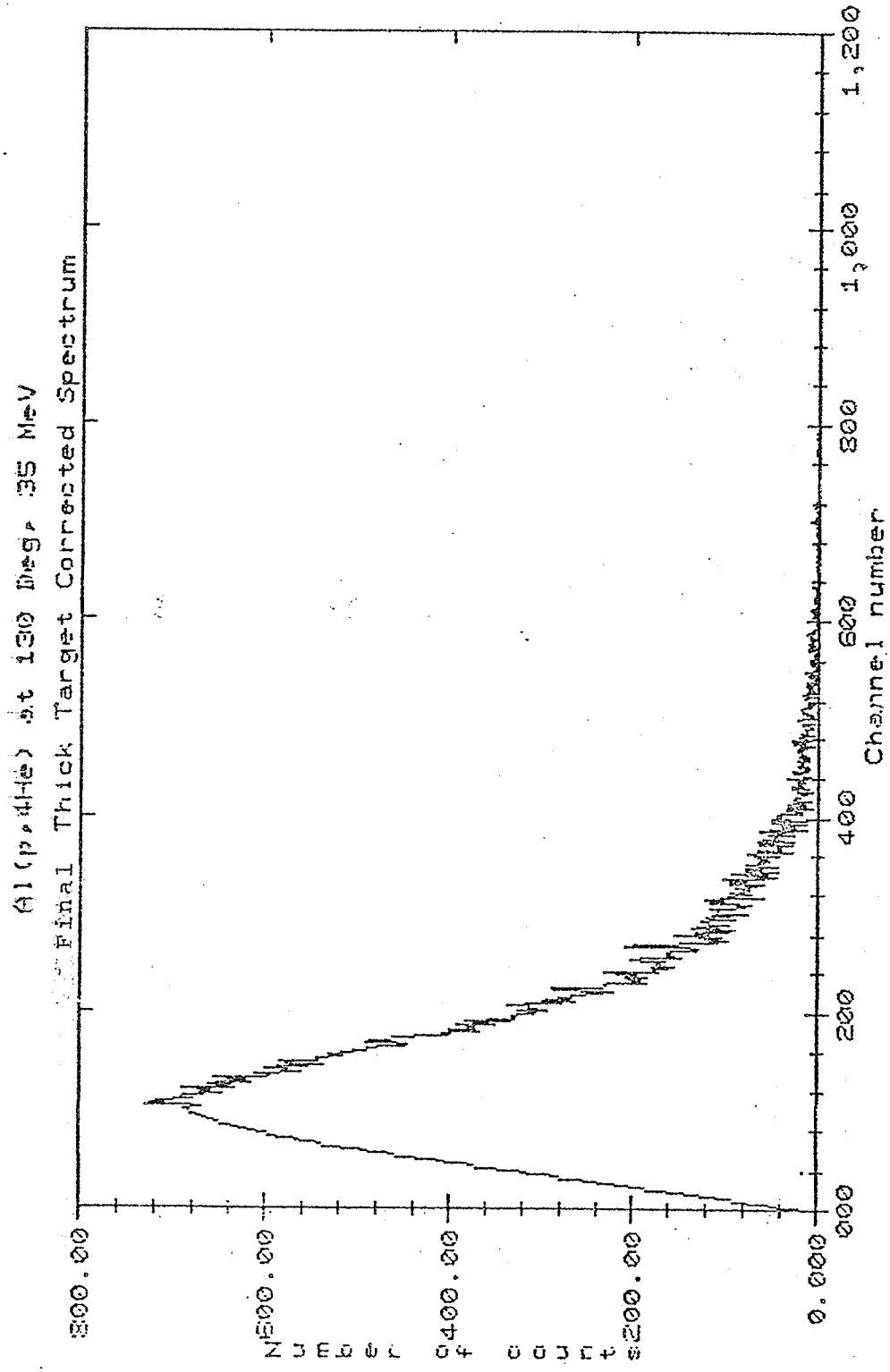
Al(p,4He) at 130 Deg. 35 MeV
Final Thick Target Corrected Spectrum
Number of counts
800.00
600.00
400.00
200.00
0.000
000
200
400
600
800
1,000
1,200
Channel number

Fig. 3-4

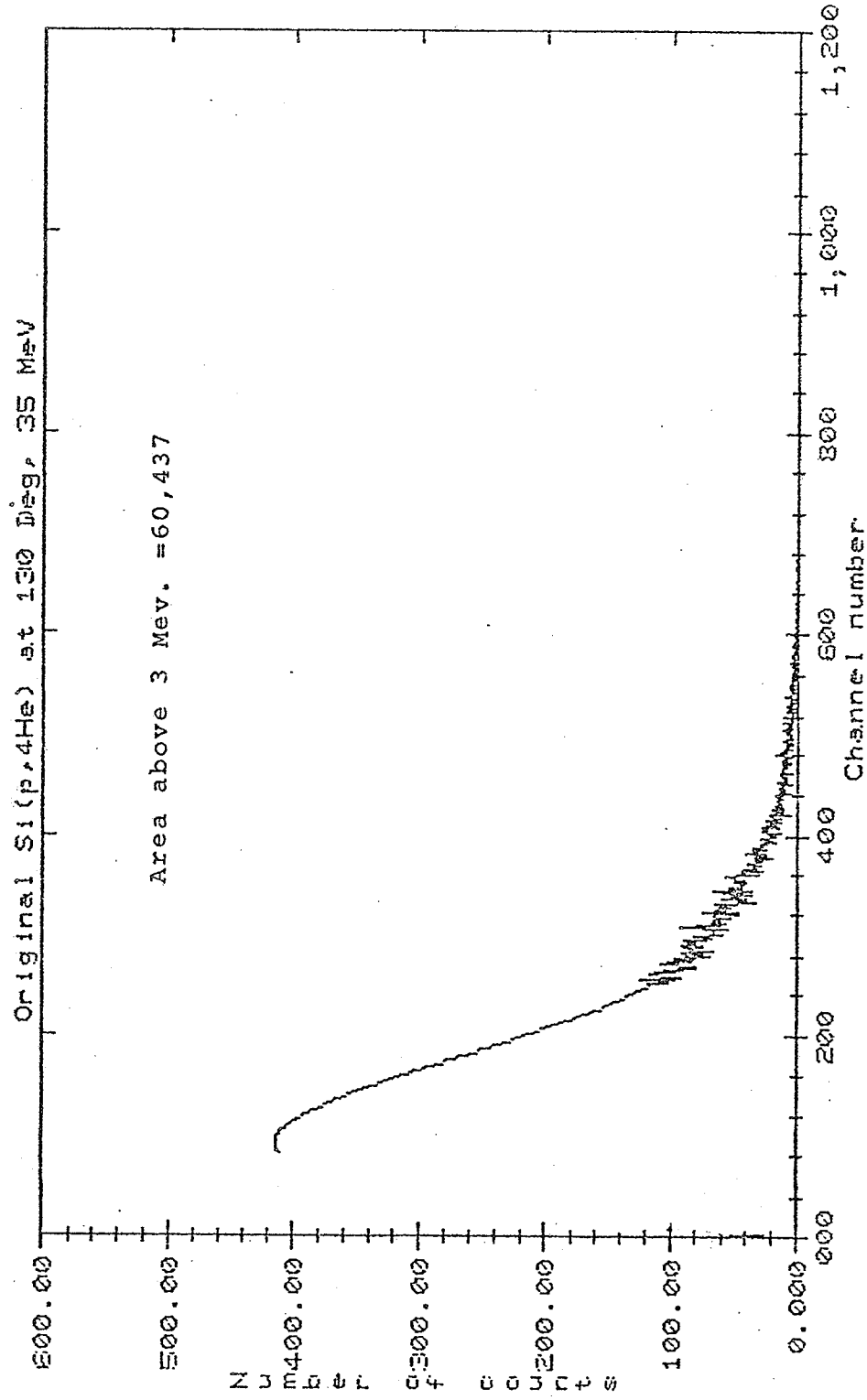

Fig. 3-5

The low energy section is a fit to the measured data which ignored the drop in counts at channel 180 due to dead layers between the detectors.

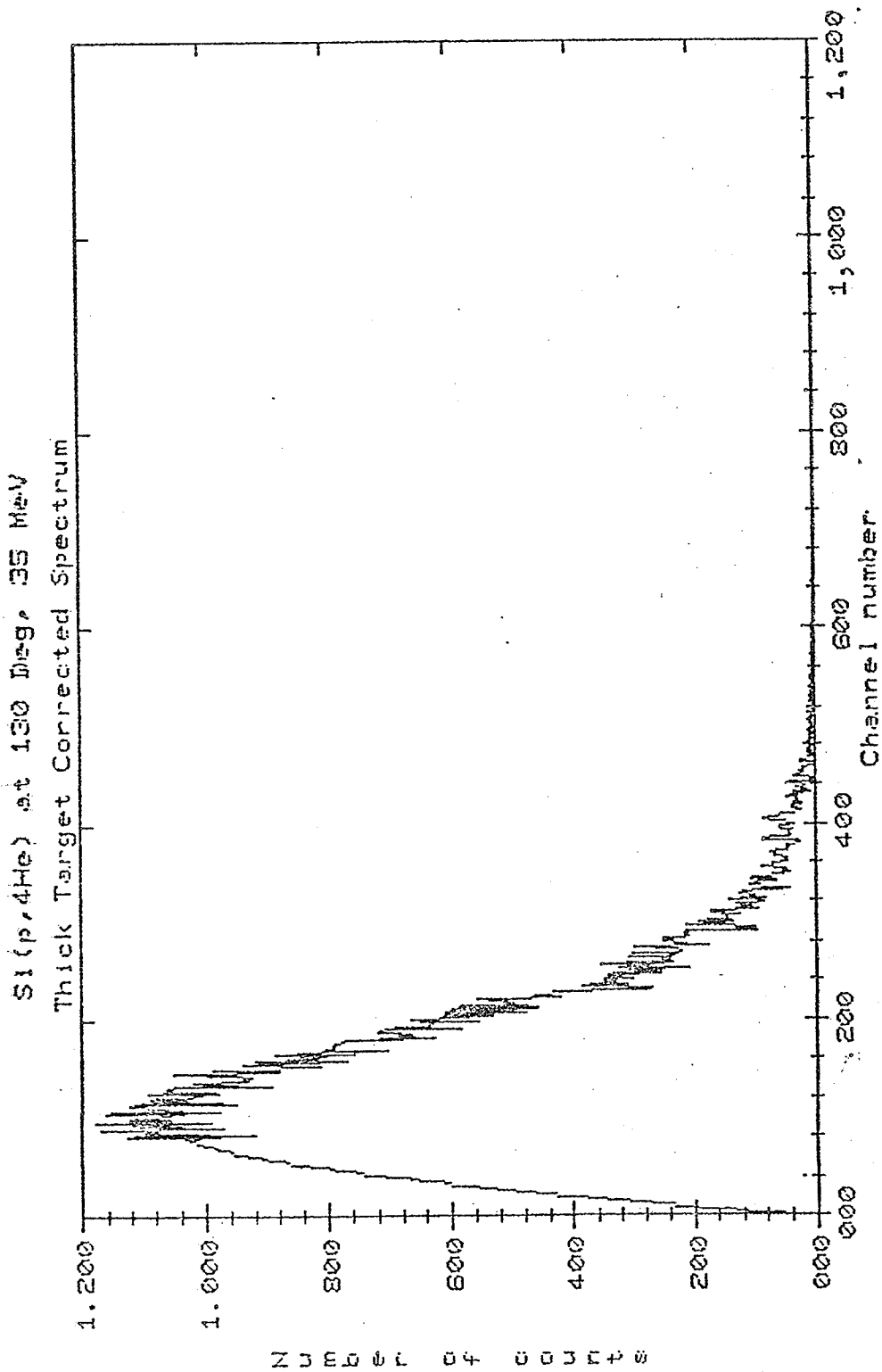
Si(p,4He) at 130 Deg. 35 MeV
Thick Target Corrected Spectrum
Channel number
0
200
400
600
800
1,000
1,200

Fig. 3-6

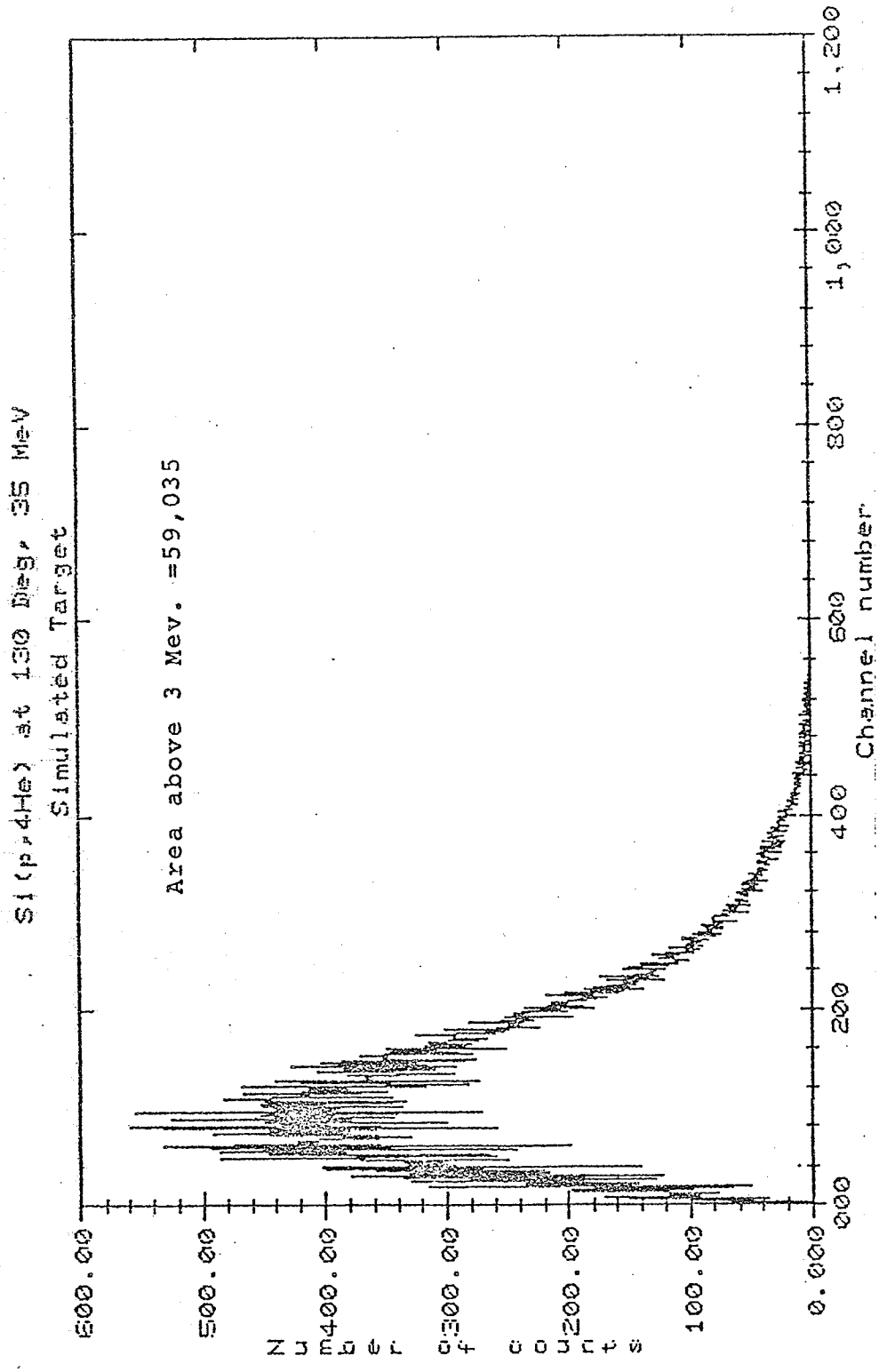
Si(p,4He) at 130 Deg, 35 MeV
Simulated Target
Area above 3 Mev. =59,035
Number of counts
Channel number
600.00
500.00
400.00
300.00
200.00
100.00
0.000
200
400
600
800
1,000
1,200

Fig. 3-7

measured spectrum in shape and size. In all cases, the error in the total number of counts is less than 3 percent.

Data with no Low Energy Measurements

Several methods were attempted to utilize the data at angles where the high energy part of the spectrum was measured but where no data were taken with the coincidence requirements removed. No data below 8 MeV exists for these angles. The part of the spectra below 8 MeV contains a large percentage of the total number of counts (over 90% at backward angles). By various methods it is possible to extrapolate the number of counts in this low energy region of the spectrum by using the available low energy data at nearby angles. However because these extrapolated areas are so large the information derived from them has such a large error that these points do not contribute to making the total cross sections more accurate. Thus the measurements at angles where no low energy data were taken were henceforth ignored. The angular dependence of the cross sections is very smooth so extrapolating and interpolating the cross sections over all angles was still accurate, using only the points where low energy data were taken.

^{3}He Analysis

No clear knowledge of the ^{3}He spectra exists below 7 MeV as the spectra with the coincidence requirements removed are swamped with alpha particles. This low energy component contains roughly fifty percent of the yield and any attempts to obtain it give considerable error. Figure 2-10 shows a typical ^{3}He spectrum. Also the ^{3}He particle yields are much lower so the statistical errors are larger than those for the alpha particle yields. Still the ^{3}He particles are also highly ionizing particles and the Si (p,^{3}He) reaction is important to the micro-electronic

applications mentioned in Chapter 1. Thus the ^{3}He data were also analyzed. The analysis was similar to the alpha particle analysis so it is not presented here.

CHAPTER IV

CROSS SECTION CALCULATIONS

Formulae

The differential cross section per unit solid angle can be expressed as:

$$\frac{d\sigma}{d\Omega} = \frac{dN}{Nn\ dx\ \Delta\Omega}$$

where $\Delta\Omega$ is the solid angle in steradians

dx is the target thickness in cm

n is the number of target nuclei per cm^3

N is the total number of incident protons

dN is the number of particles in the spectrum measured at that target angle after the correction for thick target effects.

The above formula was used to calculate the differential cross sections for all the spectra. The results are shown in Table 4-1. The angular distributions are shown in Figures 4-1 to 4-4.

To get the total (p,α) cross section one uses the relationship:[16]

$$\sigma_{tot.} = 2\pi \int_o^{\pi} \frac{d\sigma}{d\Omega} \sin\theta\ d\theta$$

The lines drawn through the data points in Figures 4-1 to 4-4 were used to extrapolate and interpolate the differential cross sections. These lines were then integrated under using the above formula to determine the total cross sections. The results are shown in Table 4-2.

The ^{3}He particle yields were calculated by the same methods as the alpha particle yields and the ($p,^3$He) cross sections are also shown in Table 4-2.

TABLE 4-1

Target	Angle	Energy	Differential Cross Section (mb/steradian)
Aluminum	15.0	45.05 ± .25	40.27
	35.0		25.42
	60.0		16.70
	90.0		14.33
	120.0		12.18
	140.0		13.40
	165.0		13.22
Silicon	15.0	45.05 ± .25	27.22
	35.0		18.39
	60.0		16.36
	90.0		11.68
	120.0		10.93
	140.0		9.75
	165.0		9.06
Aluminum	20.0	35.00 ± .25	29.27
	35.0		24.86
	50.0		19.67
	90.0		12.54
	130.0		12.73
	160.0		13.04
Silicon	20.0	35.00 ± .25	31.18
	35.0		22.02
	50.0		16.61
	70.0		14.52 ± 10%
	90.0		12.75 ± 10%
	110.0		10.65 ± 10%
	130.0		10.46
	140.0		12.36
	165.0		14.19

Errors in cross sections range from 3 to 5 percent where not shown.

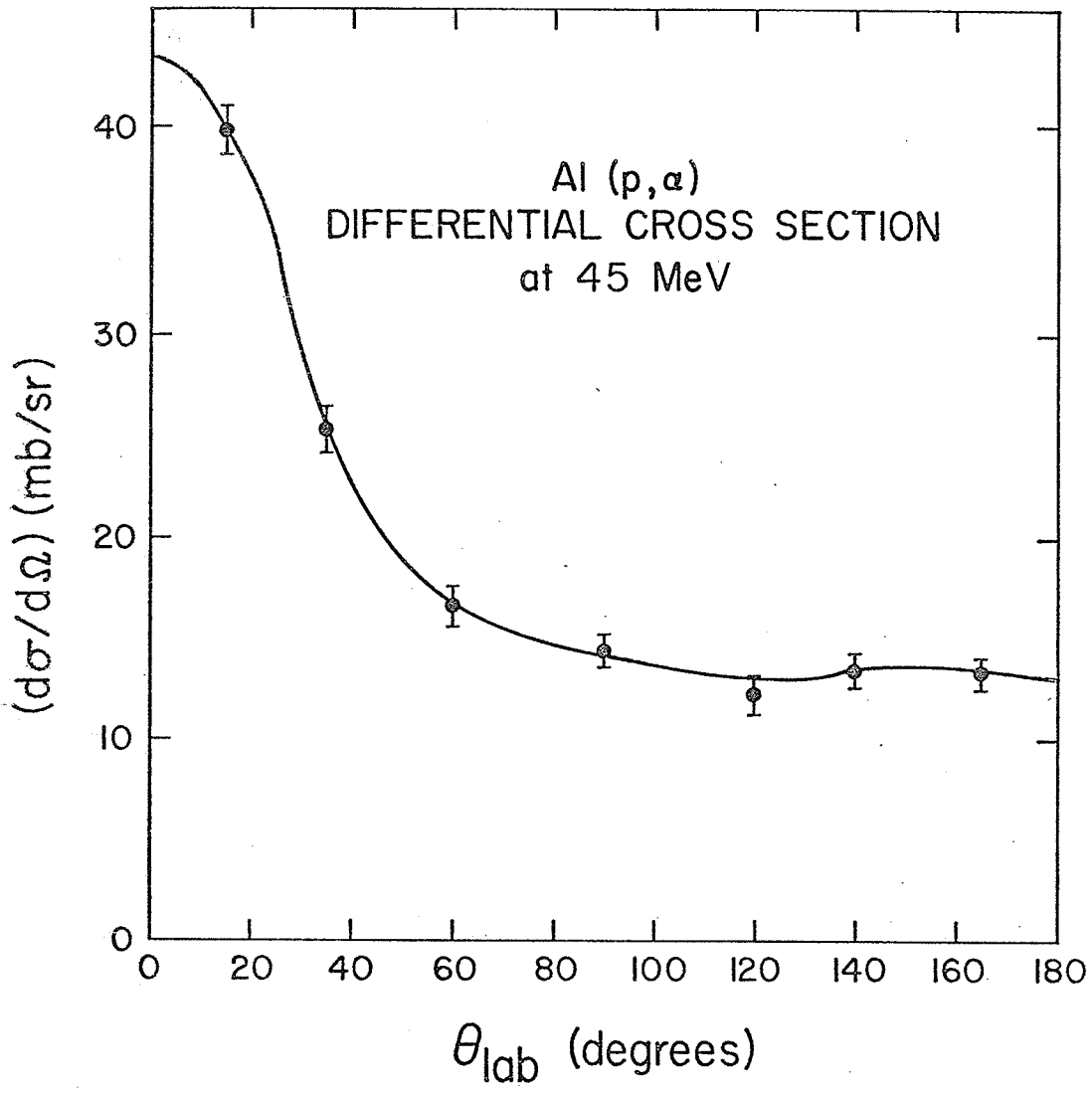
Al (p,α)
DIFFERENTIAL CROSS SECTION
at 45 MeV
(dσ/dΩ) (mb/sr)
θlab (degrees)
0
10
20
30
40
0
20
40
60
80
100
120
140
160
180

Fig. 4-1

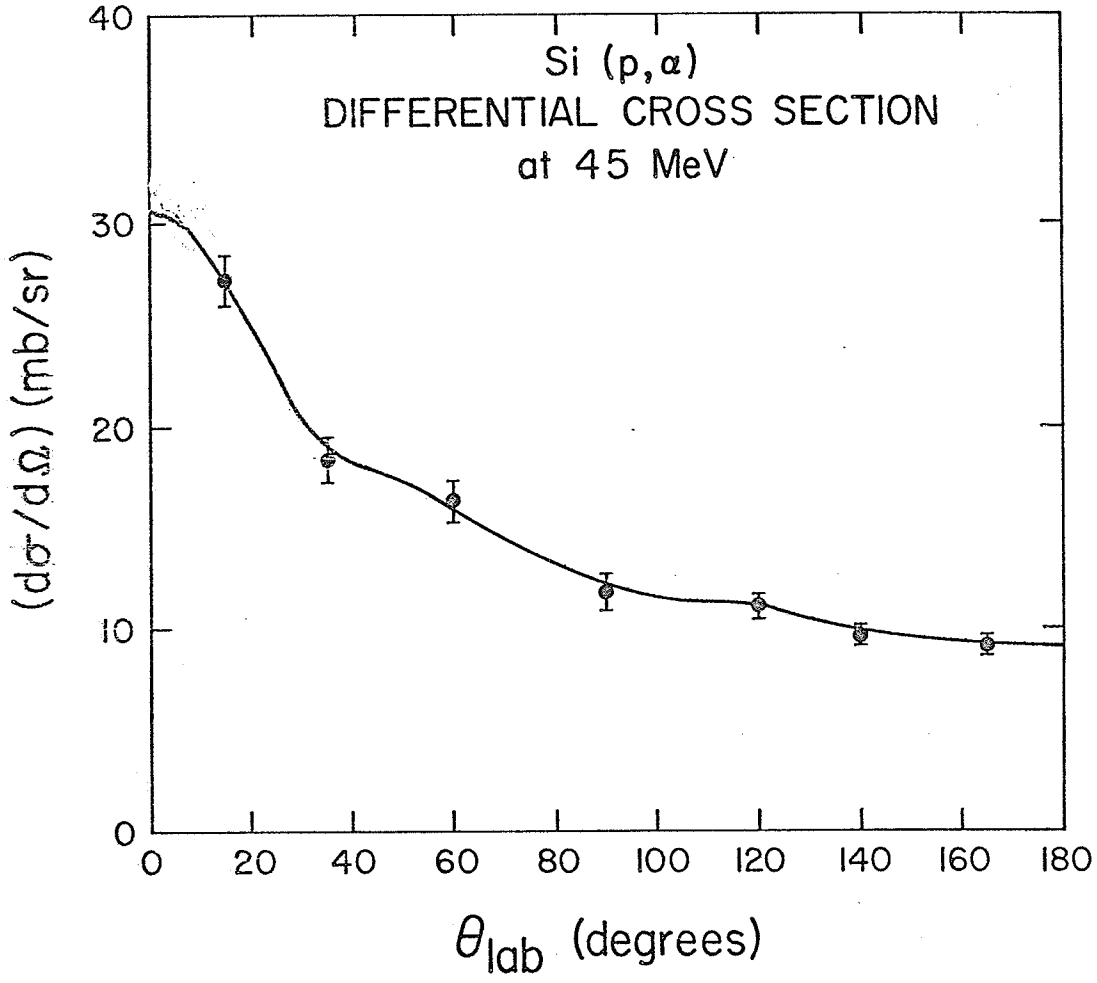
Si (p,α)
DIFFERENTIAL CROSS SECTION
at 45 MeV
(dσ/dΩ) (mb/sr)
θlab (degrees)
0
10
20
30
40
0
20
40
60
80
100
120
140
160
180

Fig. 4-2

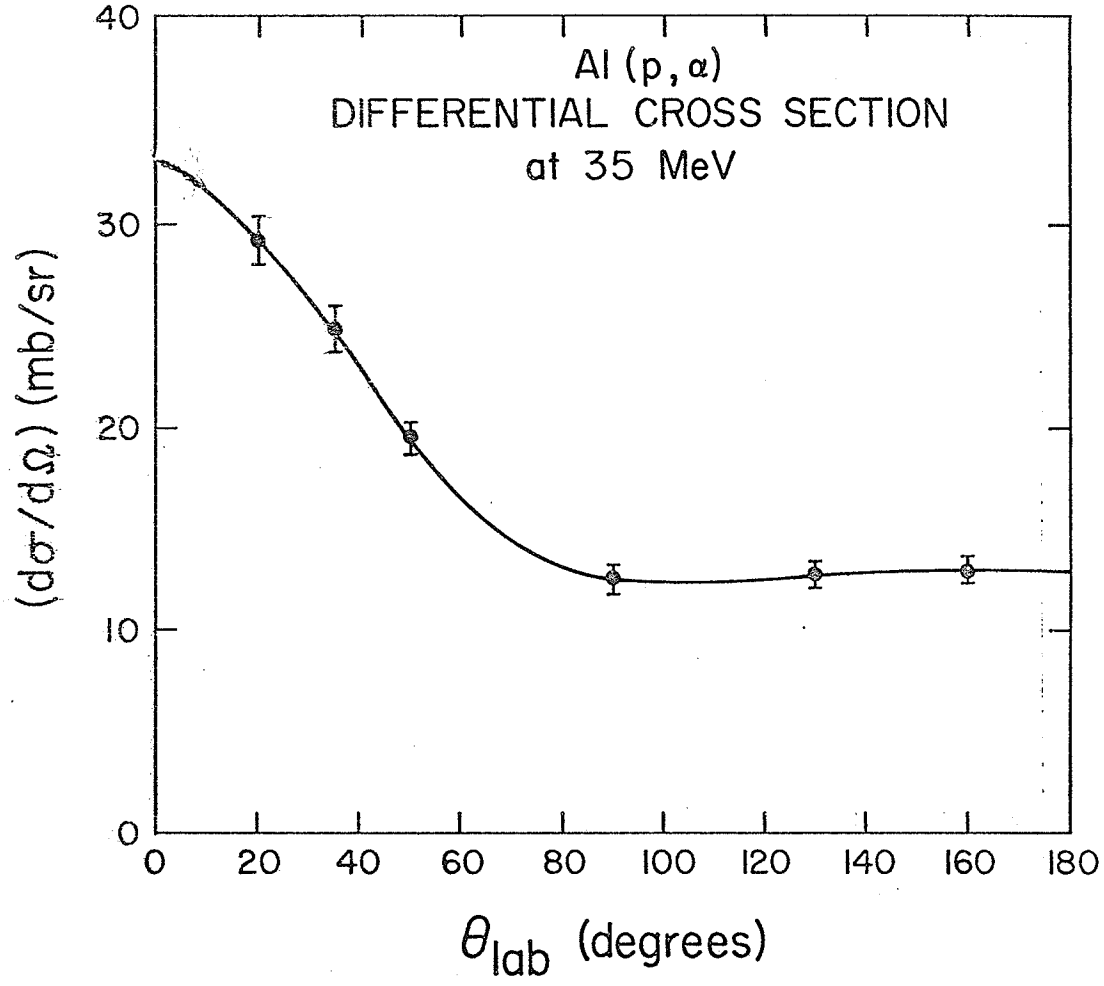
Al (p, α)
DIFFERENTIAL CROSS SECTION
at 35 MeV
(dσ/dΩ) (mb/sr)
θlab (degrees)
0
10
20
30
40
0
20
40
60
80
100
120
140
160
180

Fig. 4-3

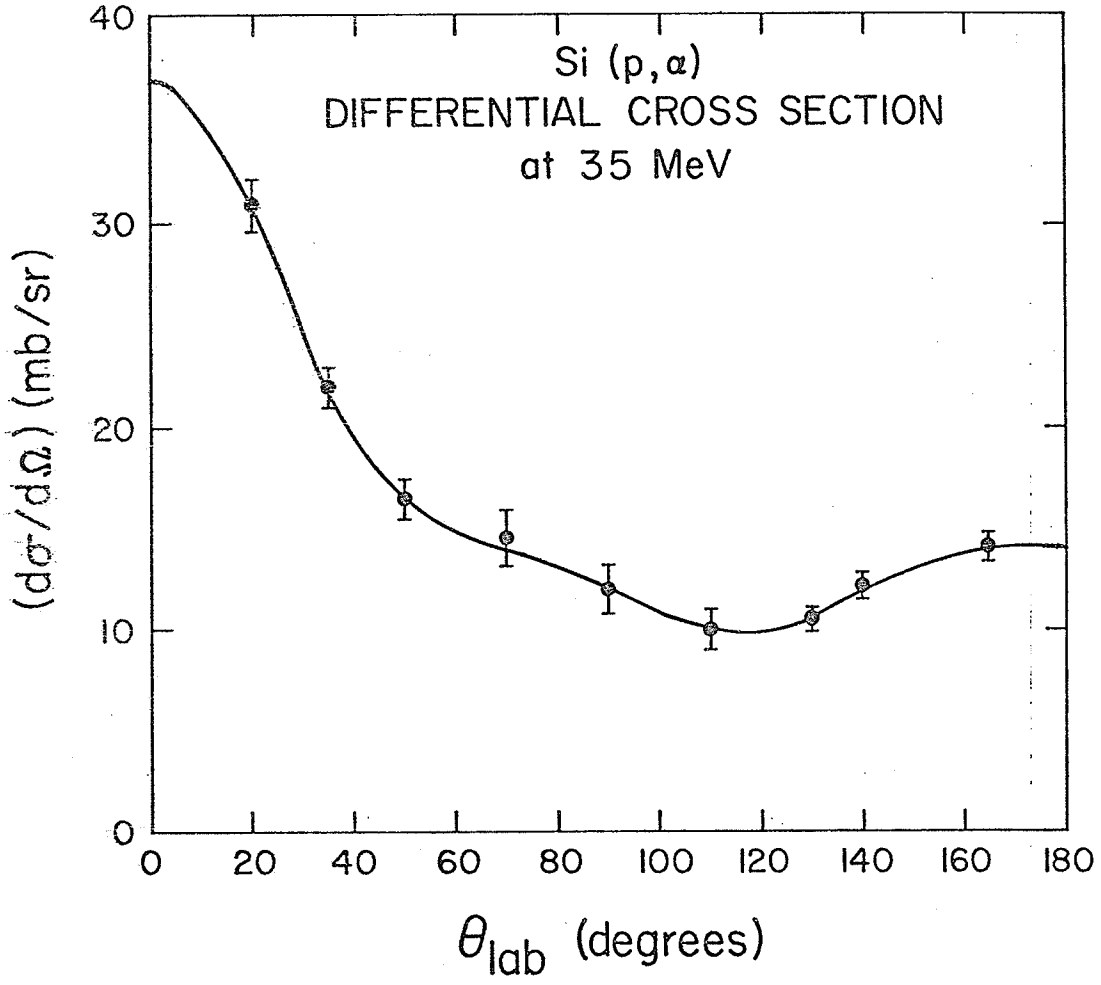
Si (p,α)
DIFFERENTIAL CROSS SECTION
at 35 MeV
(dσ/dΩ) (mb/sr)
θlab (degrees)
0
10
20
30
40
0
20
40
60
80
100
120
140
160
180

Fig. 4-4

TABLE 4-2

TOTAL REACTION CROSS SECTION

	35.00 ± .25 MeV	45.05 ± .25 MeV
Si (p, α)	180 ± 11 mb	172 ± 10 mb
^{27}Al (p, α)	195 ± 12 mb	210 ± 13 mb
Si (p, ^{3}He)	7 ± 4 mb	10 ± 5 mb
^{27}Al (p, ^{3}He)	7 ± 4 mb	10 ± 5 mb

Errors

The errors in the differential cross section data of Table 4-1 are composed of systematic and relative errors. The systematic errors include:

i) target thickness uncertainties of 0.25%

ii) solid angle uncertainties of 1.0%

iii) beam integration uncertainties of 1.0%

These errors were described in Chapter II. They affect all data points equally.

The relative errors include:

i) statistical fluctuations of less than 0.5%

ii) errors caused by the thick target correction of 3.0% for all but 3 points where the error is 7%.

iii) uncertainties caused by the dead time and background corrections of less than 0.1%.

The statistical fluctuation error was arrived at by taking the square root of the total number of counts. The thick target correction errors were calculated by testing the computer code in Chapter III. Background and deadtimes were both small as described in Chapter II.

These relative errors raise some points and lower others. The measurements made with the left and right arms were averaged together so this eliminated some of the relative error. Furthermore, even though the data points had a combined error of less than 6% the relative errors were reduced in the total cross section calculation by drawing a smooth line through the points.

The contribution to the total cross section is greater at medium angles then at very forward or backward angles (because of the sin (θ) dependence) so the error, caused by extrapolating to 0^{o} or 180^{o} is small. By analyzing various fits to the angular distributions of the differential cross sections, it was found that the uncertainty in fitting the line contributed an error of 3% to the total cross sections. This 3% when added to the systematic errors gives us a total error of 6% in the total cross sections quoted in Table 4-2.

CHAPTER V

SIGNIFICANCE OF THE RESULTS

Comparison with Existing Data

Figure 5-1 graphs the data from the present experiment along side data from previous measurements in our energy range. Figure 5-2 shows the data from the present experiment with previous data for a larger energy range. The silicon measurements clearly show good agreement with previous results[2] at 34.5 and 44.5 Mev as revealed by Table 5-1.

TABLE 5-1

A COMPARISON OF SILICON (p, α) CROSS SECTIONS

	Walton et al[2]	This work
Si (p,α)	192 ± 25 mb at 34.4 MeV	180 ± 11 mb at 35.0 MeV
Si (p,α)	167 ± 50 mb at 44.5 MeV	172 ± 10 mb at 45.0 MeV

We have reduced the errors in these measurements by a significant amount. Looking at the previous measurements, large variations in the aluminum cross sections existed with energy. These measurements range from 307 ± 40 mb for the aluminum cross section at 25.3 MeV to 71 ± 27 mb for the aluminum cross section at 38.0 MeV. If the Walton et al[2] measurements for aluminum are ignored then the aluminum cross sections also appear to have a fairly smooth energy dependence so the Walton et al measurements are the only evidence for the strong energy dependence. Unfortunately because measurements were only taken at two different energies, we have not completely resolved this matter. The silicon measurements which are the important ones for the electronic applications agree quite well and do not show much energy variation.

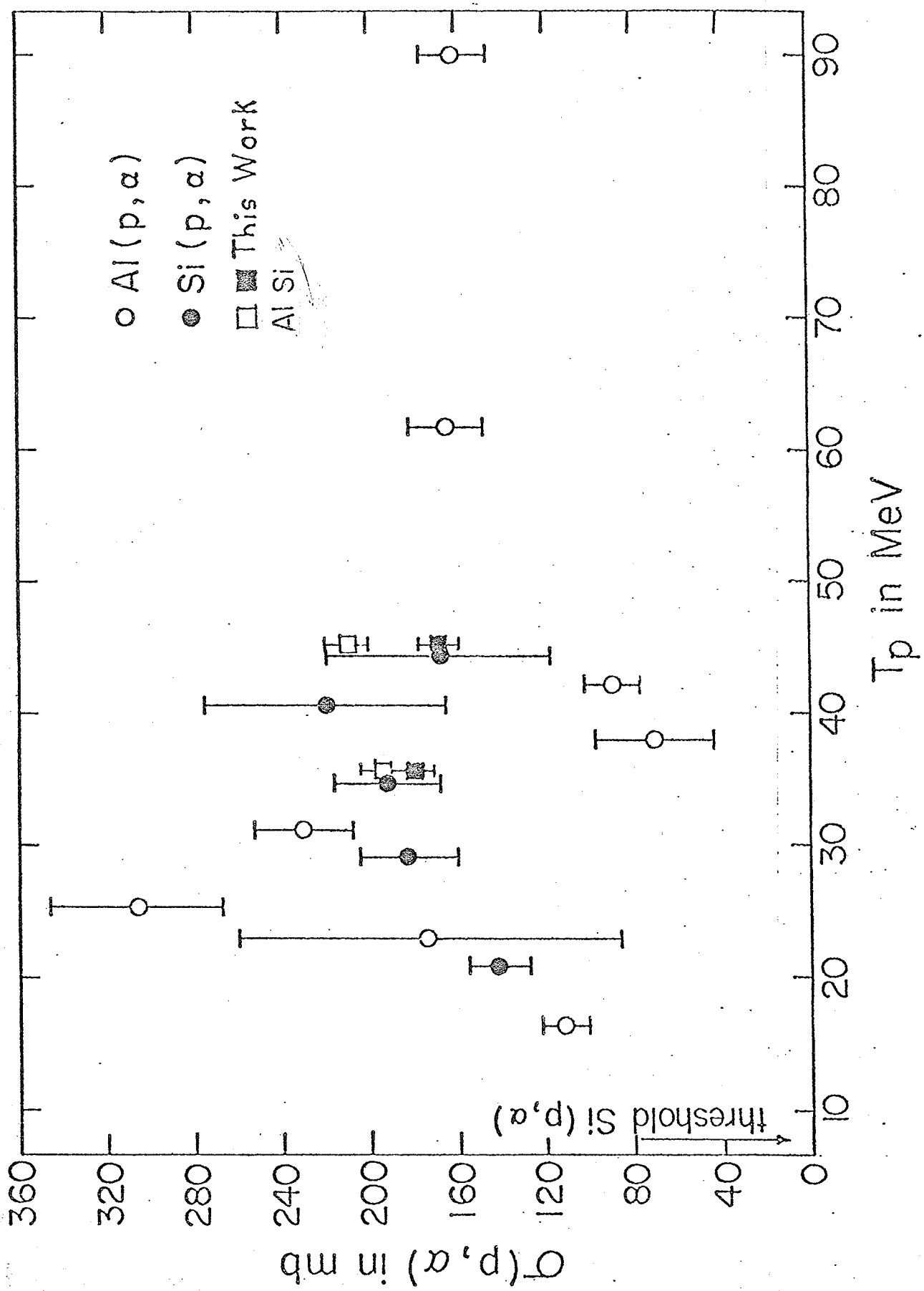
σ(p,α) in mb
Tp in MeV
o Al(p,α)
● Si(p,α)
□ ■ This Work
Al Si
threshold Si (p,α)
0
40
80
120
160
200
240
280
320
360
10
20
30
40
50
60
70
80
90

Fig. 5-1

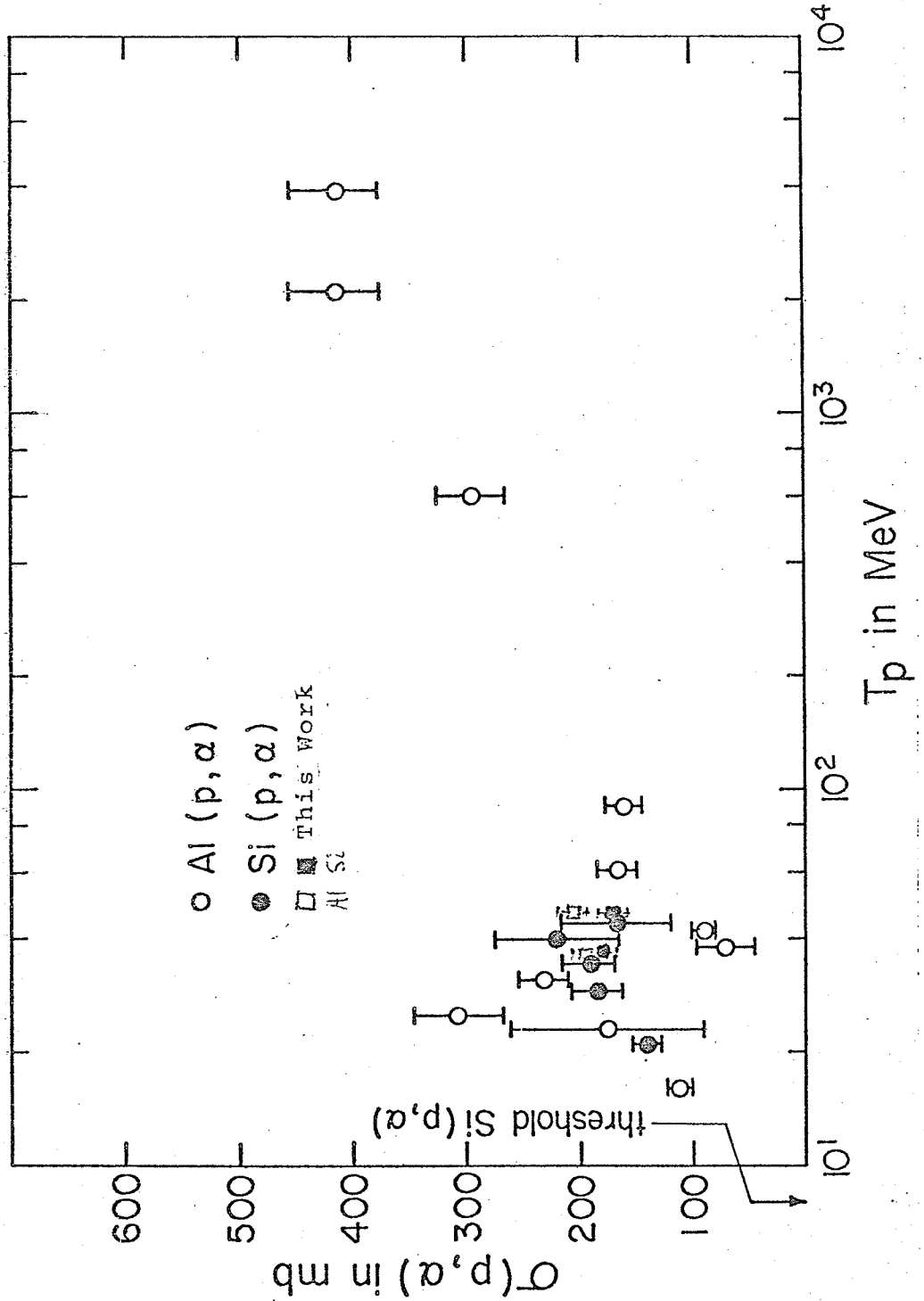
σ(p,α) in mb
600
500
400
300
200
100
threshold Si (p,α)
10¹
10²
10³
10⁴
Tp in MeV
o Al (p,α)
● Si (p,α)
□ ■ This Work

Figure 5-2

Further Discussion

The present Al (p, α) cross section measurements came out slightly higher than the Si (p, α) measurements. This can be rationalized by the fact that because of binding energy differences the aluminum reaction is energetically more favourable.

ie: $p + {}^{27}Al \rightarrow \alpha + {}^{24}Mg \qquad Q = 1.5945$ MeV

$p + {}^{28}Si \rightarrow \alpha + {}^{25}Al \qquad Q = 7.6990$ MeV

The Si (p, α) cross section is now better known at low energies. In addition to the contribution to fundamental nuclear physics these measurements have relevance to the micro-electronic and geophysical applications mentioned previously in Chapter I. Our measurements have special relevance because they were taken at energies just below the sea level cosmic ray proton peak. The cosmic ray neutron flux is higher by a factor of 500 at sea level so it is even more important to know the Si (n, α) total cross section for micro-electronic applications.

However, the nuclear force is thought to be charge independent so we can consider the (n, α) cross sections to be nearly equal to the (p,α) cross sections. Evidence for this is shown in Figure 5-3 from reference 10 which compares the ^{12}C (p, α) and (n, α) yields at similar angles (20^{o}) and energies (about 40 MeV). The resulting spectra are nearly identical in both shape and total yield. Evidently the coulomb effects of the incident proton must be small. Therefore by measuring the Si (p, α) total cross section one can at least quote a reasonable estimate for the Si (n,α) total cross section.

The final step was to convolute the energy dependence of the cross section shown on Figures 5-1 and 5-2 with the cosmic ray flux shown on Figure 1-1 and 1-2. This was done by fitting curves to the data. The

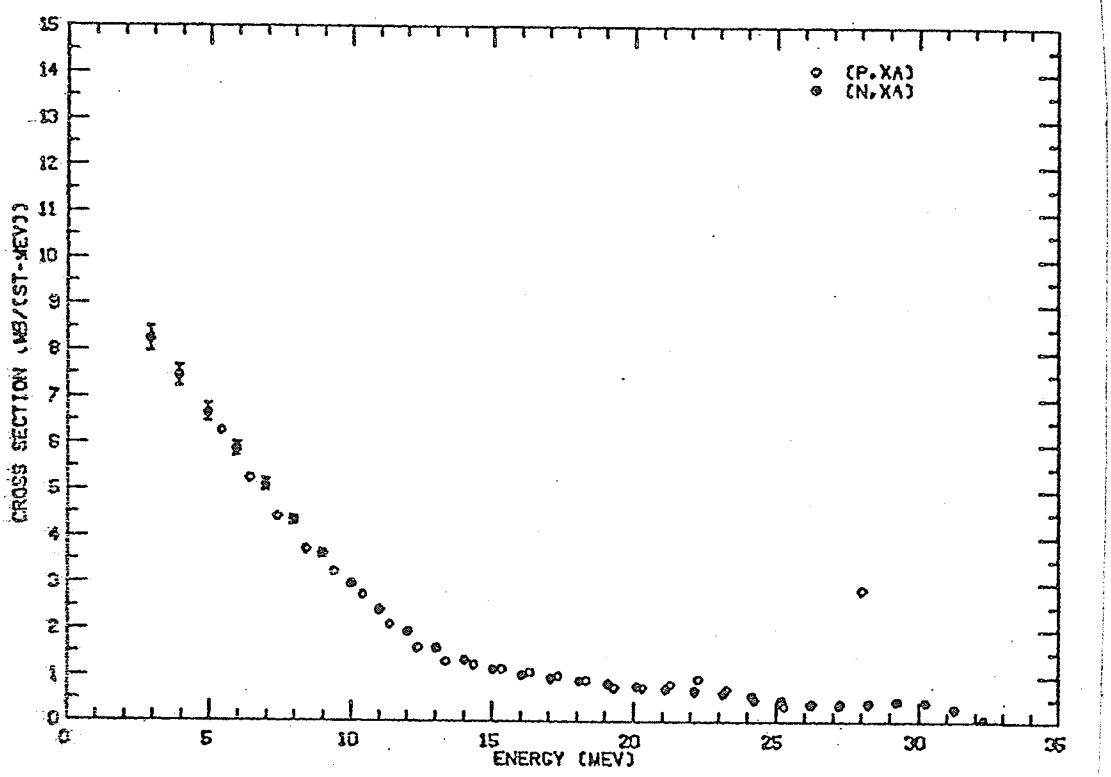

Fig. 5-3, Taken from reference (10)
A comparison of neutron and proton induced spectra for ^{12}C at 20 degrees and about 40 MeV.

aluminum cross sections were used at energies where no silicon data were available. Then the number of alpha particles produced in each cm^3 of silicon per hour is given by:

$$dN = \sum_{\text{each MeV}} F \cdot n \cdot \sigma$$

where F is the cosmic ray flux/MeV - cm^2 - hr

n is the number of target nuclei/cm^3, and

σ is the cross section in cm^2.

Table 5-2 shows the results at sea level. At higher energies the calculation was not done due to the lack of cross section data but the yield would be low because the cosmic ray flux decreases rapidly with energy. Thus at sea level with no shielding one can expect the neutron and proton components of the cosmic ray flux to produce an alpha particle in a cubic centimeter of silicon approximately every 15 hours. At an elevation of 10 Km the yield will be at least 100 times higher. With shielding such as the roof of a building, the alpha particle yield may drop considerably.

TABLE 5-2

Energy Range	Alpha yield from neutrons	Alpha yield from protons
Threshold to 100 MeV	0.033/cm^3 - hr	0.0004/cm^3 - hr
100 to 1000 MeV	0.019/cm^3 - hr	0.0010/cm^3 - hr
1 to 10 GeV	0.005/cm^3 - hr	0.0006/cm^3 - hr
Threshold to 10 GeV	0.057/cm^3 - hr	0.002/cm^3 - hr

Summary

The alpha particle spectra from protons impinging on aluminum and silicon targets were measured at 35 and 45 MeV. The silicon target was relatively thick and absorbed many low energy alpha particles. A numerical method for correcting for thick target effects has been adapted from the literature and used to correct the data. The correction technique introduced only a 3 percent error to the differential cross section data points.

The angular dependence of the differential cross sections has been determined. The angular distributions have been integrated to calculate the total cross sections for Si and Al (p,α) at 35 and 45 MeV incident proton energies. These values are accurate to 6% which is an improvement over the previous data. The silicon results agree with the measurements by Walton et al[2] at similar energies. Measurements were not taken at enough energies to conclusively state whether or not the cross sections for aluminum varied as strongly with energy as suggested by the Walton et al data. From the Si (p,α) total cross section measurements the Si (n,α) total cross sections can be inferred.

^{3}He spectra were taken during the same runs but the thickness of the delta E detectors eliminated all ^{3}He particles with energies less than 7 MeV. Thus these total reaction cross sections are not known as accurately as the alpha ones are.

The measurements made here will aid in determining the energy dependence of the Si (p,α) total reaction cross section. Once this is known, the number of alpha particles produced by cosmic ray nucleons striking silicon chips can be calculated and the corresponding failure rates of micro-electronic circuit components can be deduced. In some type of micro-electronic components, the proton and neutron fluxes can directly

cause a failure with their ionization wakes and in these chips the (p,α) and (n,α) reactions contribute only 10 percent of the total cosmic ray induced fail rate. For other types of micro-electronic components the nucleon ionization wakes are not large enough to produce failures. For these the (p,α) and (n,α) reactions form the largest computer fail rates caused by cosmic ray sources. Thus it is expected that this work will contribute to future micro-electronic research and design.

APPENDIX 1 - Polynomial Fit Program

This program was used to find range-energy relationships using Northcliffe and Schilling's tables.[13]

```
C****LEAST SQUARES AALYSIS OF POLYNOMIAL, ORDER LIMITED BY
C****DIMENSIONS ONLY
      IMPLICIT REAL*8 (A=H,O=Z)
      DIMENSION X(500),Y(500),Z(500),UA(20),UAW(20,20),
     1 VAW(20,20),A(38),B(19),XK(500),XR(500)
C****USES SUBROUTINE KINGKO TO SOLVE N BY N DETERMINENT
C****THE X AND Y INPUTS ARE THE DATA POINTS, LIMITED BY
C****DIMENSION ONLY. THE Z(I) ARE THE FITS TO THE DATA,
C****OUTPUTS X, Y, AND Z AND CONSTANTS I=NUMBER OF DATA POINTS,
C****N= NUMBER OF CONSTANTS IN POLYNOMIAL.
C***** CARD1 NO OF DATA SET
C***** CARD2 NO OF POINTS AND ORDER OF POLYNOMIAL
C***** CARD3 X AXIS AND Y AXIS
      READ (5,1111) NOSP
1111  FORMAT ( I3)
      DO 2222 LI=1,NOSP
6789  READ(5,100) I,N
100   FORMAT(2I3)
      READ(5,101) (XK(J), Y(J), J=1,I)
      DO 500 J=1,I
      XB= XK(J)
      X(J) =(XB)
500   CONTINUE
101   FORMAT (2F10.4)
      M=N-1
      M2=2*M
      DO 1 J=1,N
      DO 1 K=1,N
      UAW(J,K)=0.
      UA(J)=0.
1     VAW(J,K)=0.
      DO 5 J=1,I
      A(1)=X(J)
      INIT=1
      DO 3 L=1,M
      DO 2 K=INIT,M
      KK=K+L
      A(KK)=A(K)*A(L)
2     UAW(L+1,K+1)=UAW(L+1,K+1)+A(KK)
3     INIT=M
      UAW(2,1)=UAW(2,1+A(1)
      UAW(1,1)=UAW(1,1)+1.
      DO 4 K=1,M
4     UA(K+1)=UA(K+1)+A(K)*Y(J)
5     UA(1)=UA(1)+Y(J)
      DO 6 K=2,M
      DO 6 L=2,N
6     UAW(K+1,L-1)=UAW(K,L)
      DO 7 K=1,M
7     UAW(1,K+1)=UAW(2,K)
      DO 8 K=1,N
```

```
      DO 8 L=1,N
8     VAW(K,L)=UAW(K,L)
      CALL KINGKO  (UAW,N,DENOM)
      DO 9 K=1,N
      DO 9 L=1,N
9     UAW(K,L)=VAW(K,L)
      DO 11 K=1,N
      DO 10 L=1,N
10    UAW(L,K)=UA(L)
      CALL KINGKO  (UAW,N,DENUM)
      DO 12 KK=1,N
      DO 12 LL=1,N
12    UAW(LL,KK)=VAW(LL,KK)
11    A(K)=DENUM/DENOM
      ERROR=0.
      DO 14 K=1,I
      Z(K)=0.
      DO 13 L=1,N
13    Z(K)=Z(K)+A(L)*X(K)**(L-1)
14    ERROR=ERROR+(Z(K)-Y(K))**2
      ERROR=ERROR/FLOAT(N)
      WRITE(6,102) (X(K),Y(K),Z(K),K=1,I)
102   FORMAT((' ',3(F10.4,5X)))
      WRITE(6,103) (K,A(K),K=1,N)
103   FORMAT(' A',I2,'=',E14.8)
      WRITE(6,104) ERROR
104   FORMAT('ERROR',E14.8)
2222  CONTINUE
333   STOP
      END


      SUBROUTINE KINGKO  (UAW,NPAR,DENOM)
      IMPLICIT REAL*8 (A=H,O=Z)
C****KINGKO   - SOLVES NPAR*NPAR DETERMINENT
C****UAW=ELEMENTS OF DETERMINENT, CHANGE DIMENSION FOR MORE
C****VARIABLES.  SOLUTION OF DETERMINENT = DENOM
      DIMENSION UAW(20,20)
C****SMALL AND VLARGE PREVENT OVERFLOW AND UNDERFLOW,=0, FOR NO
C****PREVENTION
      SMALL=1.E-30
      VLARGE=1.E+40
C****SOLVES DETERMINENT BY ZEROING ELEMENTS TO RIGHT OF MAIN
C****DIAGONAL AND MULTIPLING REMAINING DIAGONAL TERMS.
C****UAW IS ALTERED IN THE SUBROUTINE
      NPER=NPAR-1
      DO 6001 KING=1,NPER
      KANG=KING+1
      DO 6002 KONG=KANG,NPAR
      IF(DABS(UAW(KING,KING)).LE.SMALL) GO TO 614
      AMULT=UAW(KING,KONG)/UAW(KING,KING)
      IF(DABS(AMULT).LE.SMALL.OR.DABS(AMULT).GE.VLARGE) GO TO 614
      DO 6003 KUNG=KING,NPAR
```

```
      IF(DABS(UAW(KUNG,KING)).LE.SMALL.OR DABS(UAW(KUNG,KING)).
     1 GE.VLARGE) GO TO 614
6003  UAW(KUNG,KONG)=UAW(KUNG,KONG)-AMULT*UAW(KUNG,KING)
6002  CONTINUE
6001  CONTINUE
      DENUM=1.
      DO 6004 KENG=1,NPAR
6004  DENOM=DENOM*UAW(KENG,KENG)
      RETURN
614   WRITE(6,100)
100   FORMAT('0UNDERFLOW IN KINGKO,   MATRIX SET =1,')
      DENOM=1.
      RETURN
      END
```

APPENDIX 2 - Data Analysis Program

This is the main data handling program which was used to do the thick target corrections.

```
      COMMON IA(1024,4),X(250),Y(250),CF(10)
      COMMON /COM1/ IB(1024,2),ILCH(5),IUCH(5),FI(2),FO(2)
      DATA RE/2HRE/,XM/2HXM/,BI/2HBI/,BO/2HBO/,EX/2HEX/,FT/2HFT/
      DATA CW/2HCW/,CS/2HCS/,SD/2HSD/,ST/2HST/,PT/2HPT/,TT/2HTT/
      DATA TA/2HTA/,CT/2HCT/,PC/2HPC/
      ASSIGN 99 TO ISTRT
      CALL ERRSET(8,ISTRT)
      NPTS=0
      ISAV=0
      CALL SETUP(NPTS,IB(1,1),IB(1,2),ISWS,MRKRS,ISUBSC)
      IREG=1024
98    IH=0
      WRITE(4,100)
      READ(3,101) COM,NUM
      IF(COM.EQ.RE) GO TO 2
      IF(COM.EQ.XM) GO TO 5
      IF(COM.EQ.CW) GO TO 10
      IF(COM.EQ.CS) GO TO 15
      IF(COM.EQ.SD) GO TO 20
      IF(COM.EQ.BI) GO TO 30
      IF(COM.EQ.BO) GO TO 40
      IF(COM.EQ.ST) GO TO 45
      IF(COM.EQ.PT) GO TO 50
      IF(COM.EQ.FT) GO TO 55
      IF(COM.EQ.TA) GO TO 58
      IF(COM.EQ.TT) GO TO 60
      IF(COM.EQ.CT) GO TO 63
      IF(COM.EQ.PC) GO TO 75
      IF(COM.EQ.EX) GO TO 90
      WRITE(4,102)
      GO TO 98
C
C     Come here to smooth the data
C     for num less than 1000 a cubic spline fit is used
C     for num GT 1000 a faster numerical method is used.
C
2     IF (NUM.GT.1000) GO TO 3
1     CALL SMOOTH(1.0,NUM)
      WRITE(4,113) NUM
      NUM=NUM+190
      IF(NUM.GT.750) GO TO 98
      GO TO 1
3     NUM=NUM-999
      DO 4 K=1,10
      YI=FLOAT(IB(NUM,1))
      DO 4 I=NUM,1000
      YNEW=(YI+2.*(FLOAT(IB(I,1)))+FLOAT(IB(I+1,1)))/4.
      YI=FLOAT(IB(I,1))
4     IB(I,1)=IFIX(YNEW)
      GO TO 98
```

```
C
5       RNUM=FLOAT(NUM)/1000.
        DO 6 I = 1,IREG
6       IB(I,1)=IFIX(RNUM*FLOAT(IB(I,1))+0.5)
        GO TO 98
C
C       Come here to clear workins arrays - IB(n,1), IB(n,2)
C
10      IF(NUM.LT.0.OR.NUM.GE.3) GO TO 80
        KK=NUM
        IF(NUM.EQ.0) KK=1
14      DO 12 I = 1,1024
12      IB(I,KK)=0
        IF(NUM.NE.0.OR.KK.EQ.2) GO TO 98
        KK=2
        GO TO 14
C
C       Come here to clear storage arrays - IA(n,J), J = 1,4
C
15      IF(NUM.LT.0.OR.NUM.GE.5) GO TO 80
        KK=NUM
        IF(NUM.EQ.0) KK=1
16      DO 17 I = 1,1024
17      IA(I,KK)=0
        IF(NUM.NE.0.OR.KK.EQ.4) GO TO 98
        KK=KK+1
        GO TO 16
C
C       Come here to stop or start display
C
20      IF(NUM.NE.0) GO TO 21
        NPTS=0
        GO TO 98
21      NPTS=IREG
        GO TO 98
C
C       Come here to read specified resion from MIRAD input file
C
30      NREG=NUM+1
        WRITE(4,103)
        READ(3,104) FI
        CALL SEEK(6,FI)
        IG=1
        IH=1
31      READ(6) N1,N2,N3
        IF(N1.EQ.IREG) GO TO 32
        WRITE(4,105) N1,IREG
        GO TO 99
32      K1=1
        DO 34 I =1,N2
        K2=K1+N3-1
        IF(I.EQ.N2) K2=N1
        READ(6) L1,L2,(IB(M,1), M=K1,K2)
```

```
      IF(L1.NE.K1.OR.L2.NE.K2) GO TO 38
      K1=K2+1
34    CONTINUE
      IF(IG.EQ.NREG) GO TO 36
      IG=IG+1
      GO TO 31
38    WRITE(4,114) L1,L2,K1,K2
36    GO TO 99
C
C     Come here to write MIRAD compatible output file
C
40    IF(NUM.LT.1.OR.NUM.GT.4) GO TO 80
      WRITE(4,106)
      READ(3,104) FO
      CALL ENTER(7,FO)
      IH=2
      N1=IREG
      N3=70
      N2=(N1+N3-1)/N3
      DO 42 I = 1,NUM
      WRITE(7) N1,N2,N3
      K1=1
      DO 44 J = 1,N2
      K2=K1+N3-1
      IF(J.EQ.N2) K2=N1
      WRITE(7) K1,K2,(IA(KI,I), KI=K1,K2)
      K1=K2+1
44    CONTINUE
42    CONTINUE
      CALL CLOSE(7)
      GO TO 98
C
C     Come here to store fitted array - IB(n,2) - in the array
C     IA(n,J) where J is specified by NUM
C
45    IF(NUM.LT.1.OR.NUM.GE.5) GO TO 80
      DO 47 I = 1,IREG
47    IA(I,NUM)=IB(I,2)
      WRITE(4,107) NUM
      GO TO 98
C
C     Come here to specify points for generating polynomial fit
C
50    IF(NUM.LT.1.OR.NUM.GT.5) GO TO 80
      WRITE(4,119)
      READ(3,120) RL
      NRL=IFIX(((RL/0.001291)**0.5847953216)/0.045924328)
      NRLP1=NRL+1
      LL=1
      WRITE(4,108)
      DO 51 I = 1,NUM
      READ(3,109) ILCH(I), IUCH(I)
      IPT=IUCH(I)-ILCH(I)
      LU=LL+IPT
```

```
      LX=ILCH(I)-1
      DO 53 J = LL,LU
      LX=LX+1
      X(J)=FLOAT(LX+NRL)
53    Y(J)=FLOAT(IB(LX,1))
      LL=LU+1
51    CONTINUE
      ISAV=LL-1
      ISCH=IUCH(NUM)+NRL
      GO TO 98
C
C     Come here to fit polynomial and generate additional data
C
55    IF(NUM.LT.1.OR.NUM.GT.10) GO TO 80
      IF(ISAV.NE.0) GO TO 56
      WRITE(4,110)
      GO TO 98
56    MP=NUM
      CALL POLFIT(ISAV,MP,CHISQR,1)
      DO 57 I =NRLP1,ISCH
      Z=FLOAT(I)
      R=CF(MP)*Z
      IF(MP.EQ.1) GO TO 57
      M1=MP
      JM=MP-1
      DO 52 J = 1,JM
      M1=M1-1
52    R=(R+CF(M1))*Z
      INRL=I-NRL
57    IB(INRL,2)=IFIX(R+0.5)
      ISAV=0
      GO TO 98
C
C     Come here to transfer array IB(n,1) to IB(n,2) from n = NUM to IREG
C
58    DO 59 I = NUM,IREG
59    IB(I,2)=IB(I,1)
      GO TO 98
C
C     Come here to output data on terminal
C
60    IF(NUM.LT.0.OR.NUM.GE.3) GO TO 80
      KK=NUM
      IF(NUM.EQ.0) KK=1
      LIM=IREG/8
61    WRITE(4,111) KK
      K1=1
      DO 62 I = 1,LIM
      K2=K1+7
      WRITE(4,112) (IB(J,KK), J=K1,K2)
      K1=K2+1
62    CONTINUE
      IF(NUM.NE.0.OR.KK.EQ.2) GO TO 98
      KK=2
```

```
      GO TO 61
C
C     COME HERE TO DO THICK TARGET CORRECTION
C
63    WRITE(4,119)
      READ(3,120)RL
      CALL THICK (SC,RT,NUM,RL)
      GO TO 98
C
75    DO 76 I=NUM,900
76    IB(I,1)=IB(NUM,1)
      GO TO 98
C     This is an error condition, the value of NUM is illegal
C
80    WRITE(4,113) NUM
      GO TO 98
C
C     Come here on receiving CNTRL P
C
99    IF(IH.EQ.1) CALL CLOSE(6)
      IF(IH.EQ.2) CALL CLOSE(7)
      GO TO 98
90    STOP
100   FORMAT(' ENTER COMMAND')
101   FORMAT(A2,I5)
102   FORMAT(' ILLEGAL COMMAND, TRY AGAIN')
103   FORMAT(' ENTER INPUT FILENAME')
104   FORMAT(A5,A4)
105   FORMAT(' SPECIFIED REGION SIZE DISAGREES WITH THAT ON INPUT FILE'/
     1  ' SPECIFIED REGION SIZE',I5/' SIZE FROM INPUT FILE',I5)
106   FORMAT(' ENTER OUTPUT FILENAME')
107   FORMAT(' DATA SAVED IN REGION',I2)
108   FORMAT(' ENTER FIRST AND LAST CHANNEL NOS. FOR EACH SET OF',
     1  ' SEQUENTIAL POINTS TO BE FITTED - I5/I5')
109   FORMAT(I5/I5)
110   FORMAT(' NO POINTS SPECIFIED FOR FITTING')
111   FORMAT(' ARRAY',I2)
112   FORMAT(5X,8I8)
113   FORMAT(' VALUE OF NUM,',I5,', IS ILLEGAL')
114   FORMAT(' COMMAND ABORTED, TAPE AND CALCULATED PARAMETERS DISAGREE'/
     1  ' TAPE',2I5/' CALCULATED',2I5)
115   FORMAT('ENTER CONSTANTS FOR SCALE AND INTERCEPT')
116   FORMAT(I5,I5)
117   FORMAT(' ENTER THE ',I5,' COEFFICIENTS')
118   FORMAT(F10.7)
119   FORMAT(' ENTER THE TARGET THICKNESS IN MM')
120   FORMAT(F8.5)
      END
```

```
      SUBROUTINE THICK(SC,RT,NUM,RL)
      COMMON IA(1024,4),X(250),Y(250),CF(10)
      COMMON /COM1/ IB(1024,2),ILCH(5),IUCH(5),FI(2),FO(2)
      C8=0.28031047
      C1=0.54906892
      C2=0.12366895
      C3=-0.0019611173
      C4=0.71534988/10000.
      C5=-0.19288997/100000.
      C6=0.29340044/10000000.
      C7=-0.18608327/1000000000.
      D1=-0.067805901
      D2=0.70569595
      D3=0.67189260
      D4=-0.37791931
      D5=0.092570545
      D6=-0.011951416
      D7=0.83186985/1000.
      D8=-0.29182159/10000.
      D9=0.40028288/1000000.
      DO 70 I=1,900
      RJ=FLOAT(901-I)*0.0542918
      J=901-I
      IF(IB(J,2).EQ.0) GO TO 70
      R=C1*RJ+C2*RJ*RJ+C3*(RJ**3.)+C4*(RJ**4.)+C8
      R=R+C5*(RJ**5.)+C6*(RJ**6.0)+C7*(RJ**7.)
      RPL=R+RL
      DRJ=C1+2.*C2*RJ+3.*C3*RJ*RJ+4.*C4*(RJ**3.)
      DRJ=DRJ+5.*C5*(RJ**4.)+6.*C6*(RJ**5.)+7.*C7*(RJ**6.)
      D2R=2.*C2+6.*C3*RJ+12.*C4*RJ*RJ+20.*C5*(RJ**3.)
      D2R=D2R+30.*C6*(RJ**4.)+42.*C7*(RJ**5.)
      E=D1+D2*R+D3*(R**2.)+D4*(R**3.)+D5*(R**4.)+D7*(R**6.)
      E=E+D6*(R**5.)+D8*(R**7.)+D9*(R**8.)
      EPL=D1+D2*RPL+D3*(RPL**2.)+D7*(RFL**6.)+D8*(RPL**7.)
      EPL=EPL+D4*(RPL**3.)+D5*(RPL**4.)+D6*(RFL**5.)+D9*(RPL**8.)
      RK=RJ+EPL-E
      K=IFIX(RK/0.0542918)
      DV=0.
      DRK=C1+2.*C2*RK+3.*C3*RK*RK+4.*C4*(RK**3.)
      DRK=DRK+C5*5.*(RK**4.)+6.*C6*(RK**5.)+7.*C7*(RK**6.)
      IF(IB(J,2).EQ.0) GO TO 69
      IF(J.GT.2) GO TO 68
      GO TO 69
68    DO 67 II=1,1
67    DV=DV+FLOAT(IB((J+II),1)-IB((J-II),1))/2.0
      DV=DV/0.0542918
69    P=RL*(FLOAT(IB(J,2))*D2R/(DRJ**2.)-DV/DRJ)+FLOAT(IB(K,2))*DRJ/DRK
      IB(J,2)=IFIX(P)
70    IF(IB(J,2).LT.0) IB(J,2)=0
      RETURN
      END
```

```
      SUBROUTINE POLFIT (NPTS,NTERMS,CHISQR,LN)
      DOUBLE PRECISION SUMX,SUMY,XTERM,YTERM,ARRAY,CHISQ
      DIMENSION SUMX(19),SUMY(10),ARRAY(10,10)
      COMMON IA(1024,4),X(250),Y(250),A(10)
C
C        ACCUMULATE WEIGHTED SUMS
C
      KV=1
      WRITE(4,400) NPTS
400   FORMAT(2X,I5,' POINTS USED IN FIT')
      JER=NPTS/8 + 1
      DO 250 I = 1,JER
      KW=KV+7
      IF(I.EQ.JER) KW=NPTS
      WRITE(4,300)  (X(LV),LV=KV,KW)
      WRITE(4,300)  (Y(LV),LV=KV,KW)
      WRITE(4,305)
      KV=KW+1
250   CONTINUE
300   FORMAT(2X,8F8.1)
305   FORMAT(/)
      LM=2*LN
11    NMAX = 2*NTERMS - 1
      DO 13 N=1,NMAX
13    SUMX(N)=0.
      DO 15 J=1,NTERMS
15    SUMY(J)=0.
      CHISQ=0.
21    DO 50 I=1,NPTS
      XI=X(I)
      YI=Y(I)
      WEIGHT=1./YI
      XTERM=WEIGHT*(XI**LM)
      DO 44 N=1,NMAX
      SUMX(N)=SUMX(N)+XTERM
44    XTERM=XTERM*XI
45    YTERM=WEIGHT*YI*(XI**LN)
      DO 48 N=1,NTERMS
      SUMY(N)=SUMY(N)+YTERM
48    YTERM=YTERM*XI
49    CHISQ=CHISQ+WEIGHT*YI**2
50    CONTINUE
      WRITE(4,301) LN,NTERMS
301   FORMAT(' FIT INCLUDES TERMS FROM X**',I1,' TO X**',I1)
      WRITE(4,302)
302   FORMAT(' COEFFICIENTS ARE')
C
C        CONSTRUCT MATRICES AND CALCULATE COEFFICIENTS
C
51    DO 54 J=1,NTERMS
      DO 54 K=1,NTERMS
      N=J+K-1
54    ARRAY(J,K)=SUMX(N)
      DELTA=DETERM (ARRAY,NTERMS)
      IF(DELTA) 61,57,61
```

```
57      CHISQR=0.
        DO 59 J=1,NTERMS
59      A(J)=0.
        GO TO 80
61      DO 70 L=1,NTERMS
62      DO 66 J=1,NTERMS
        DO 65 K=1,NTERMS
        N=J+K-1
65      ARRAY(J,K)=SUMX(N)
66      ARRAY(J,L)=SUMY(J)
        A(L)=DETERM(ARRAY,NTERMS)/DELTA
        WRITE(4,303) L,A(L)
70      CONTINUE
303     FORMAT(2X,I2,F12.7)
C
C          CALCULATE CHI SQUARE
C
71      DO 75 J=1,NTERMS
        CHISQ=CHISQ-2.*A(J)*SUMY(J)
        DO 75 K=1,NTERMS
        N=J+K-1
75      CHISQ=CHISQ+A(J)*A(K)*SUMX(N)
76      FREE=NPTS-NTERMS
77      CHISQR=CHISQ/FREE
        WRITE(4,304) CHISQR
304     FORMAT(' REDUCED CHISQ IS',F12.3)
80      RETURN
        END


        SUBROUTINE SMOOTH(PP,IC)
        REAL X(200),U(200),Y(200),Y2(200),DX(200),P(200)
        COMMON/PPP/A(200),B(200),C(200),D(200)
        COMMON /COM1/ IB(1024,2)
        NPTS=200
        DO 1 I=1,NPTS
        P(I)=PP
        U(I)=FLOAT(IB(IC+I,1))
1       X(I)=I
        Y2(1)=Y2(NPTS)=0.
        CALL FLATC(NPTS,X,U,P,Y,Y2,DX)
        DO 2 J=1,NPTS
        U(J)=D(J)
2       IB(IC+J,1)=IFIX(U(J))
        RETURN
        END
```

```
      SUBROUTINE FLATC(N,X,U,P,Y,Y2,DX)
      DIMENSION X(2),U(2),P(2),Y(2),Y2(2),DX(2)
      COMMON/PPP/A(200),B(200),C(200),D(200)
      WW=1.
      WW1=0.
      N1=N-1
      N2=N-2
      C(1)=0.
      D(1)=0.
      RR1=Y2(1)
      RR2=Y2(N)
      B(1)=0.
      B(N)=0.
      DX(N)=1.
      H1=X(2)-X(1)
      DX(1)=H1
      DO 1 K=2,N1
           H2=X(K+1)-X(K)
           DX(K)=H2
           D(K)=1./(2.*(H1+H2)-H1*H1*D(K-1))
           H1=H2
1     CONTINUE
2     DO 3 K=1,N
           Y2(K)=0.
           Y(K) =U(K)
3     CONTINUE
4     W=WW
      W1=1.-W
      DO 6 K=1,N1
           H2=DX(K)
           R2=(Y(K+1)-Y(K))/H2
           IF(K.EQ.1) GO TO 5
           H=6.0*(R2-R1)
           IF(K.EQ.2) H=H-H1*B(1)
           IF(K.EQ.N1) H=H-H2*B(N)
           C(K)=D(K)*(H-H1*C(K-1))
5          H1=H2
           R1=R2
6     CONTINUE
      B(N1)=C(N1)
      IF(N1.LE.2) GO TO 8
      DO 7 J=2,N2
           K=N-J
           B(K)=C(K)-D(K)*DX(K)*B(K+1)
7     CONTINUE
8     DO 9 K=2,N1
           B(K)=W*B(K)+W1*Y2(K)
9     CONTINUE
      J1=1
      H5=0.
      DO 10 K=1,N
```

```
          J2=K+1
          IF(K.EQ.N) J2=N
          H=((B(J2)-B(K))/DX(K)-(B(K)-B(J1))/DX(J1))/P(K)
          IF(W.EQ.1.) A(K)=-H
          IF(W.NE.1.) A(K)=W*(U(K)-H)+W1*Y(K)
          H5=H5+ABS(A(K))
          J1=K
10      CONTINUE
        H5=1./H5
        IF(W.NE.1.) GO TO 13
        H1=0.
        H2=0.
        DO 11 K=1,N
           H=Y(K)
           H1=H1+A(K)*H
            H2=H2+H*H
11      CONTINUE
        WW2=H1/H2
        IF(ABS(WW2-WW1).LT.5.E-4*ABS(WW2)) GO TO 12
        WW1=WW2
        GO TO 15
12      WW=2./(1.+SQRT(1.-WW2))
        B(1)=RR1
        B(N)=RR2
        GO TO 2
13      H2=0.
        H3=0.
        H4=0.
        DO 14 K=1,N
          H2=H2+ABS(A(K)-Y(K))
          H3=H3+ABS(B(K))
          H4=H4+ABS(B(K)-Y2(K))
14      CONTINUE
        IF(H2*H5+H4/H3.LT.5.E-4) GO TO 17
        H5=1.
15      DO 16 K=1,N
          Y2(K)=B(K)
        Y(K) =A(K)*H5
16      CONTINUE
        GO TO 4
17      DO 18 K=1,N1
          J2=K+1
          D(K)=A(K)
          A(K)=(B(J2)-B(K))/(6.*DX(K))
          C(K)=(A(J2)-D(K))/DX(K)-DX(K)*(B(J2)+2.*B(K))/6.
          B(K)=.5*B(K)
18      CONTINUE
        D(N)=A(N)
        B(N)=.5*B(N)
        RETURN
        END
```

APPENDIX 3 - Test Of Thick Target Correction

This subroutine was used to determine the accuracy of the thick target correction.

```
      SUBROUTINE THICK(RL)
      REAL Z(800)
      COMMON /COM1/ IB(1024,2),ILCH(5),IUCH(5),FI(2),FO(2)
      D8=0.28031047
      D1=0.54906892
      D2=0.12366895
      D3=-0.0019611173
      D4=0.000071534988
      D5=-0.19288997/100000.
      D6=0.29340044/10000000.
      D7=-0.18608327/1000000000.
      C1=-0.067805901
      C2=0.70569595
      C3=0.6718926
      C4=-0.37791931
      C5=0.092570545
      C6=-0.011951416
      C7=0.83186985/1000.
      C8=-0.29182159/10000.
      C9=0.40028288/1000000.
      DO 80 J=1,675
      Z(J)=0.
      K=0
      IF(IB(J,1).EQ.0) GO TO 80
      RJ=FLOAT(J)*0.037445
      RIB=FLOAT(IB(J,1))
      DO 70 I=1,20
      RI=20.5-FLOAT(I)
      T=RI*RL/20.0
      R=D8+D1*RJ+D2*RJ*RJ+D3*(RJ**3.)+D4*(RJ**4.)
      R=R+D5*(RJ**5.)+D6*(RJ**6.0)+D7*(RJ**7.)
      RO=R-T
      IF(RO.LT.0) GO TO 70
      E=C1+C2*RO+C3*(RO**2.)+C4*(RO**3.)+C5*(RO**4.)
      E=E+C6*(RO**5.)+C7*(RO**6.)+C8*(RO**7.)+C9*(RO**8.)
      K=IFIX(E/0.037445)
      IF(K.GT.J) K=J
      Z(K)=Z(K)+RIB/20.0
70    CONTINUE
80    CONTINUE
      DO 90 I=1,666
90    IB(I,2)=IFIX(Z(I))
      RETURN
      END
```

References

1) J.F.Ziegler and W.A.Lanford, Science 206,776 (1979).

2) J.R.Walton, A.Yaniv, D.Heymann, D.Edgerley, and M.W.Rowe, J. Geophysical Research 78, 6428 (1973) and Ibid 79, 314 (1974).

3) C.B.Fulmer, and B.L.Cohen, Phys. Rev. 112, 1675 (1958).

4) F.E.Bertrand and R.W.Peelle, Phys. Rev. C8, 1045 (1973).

5) J.R.Wu, C.C.Chang, and H.D.Holmgren, Phys. Rev. C19, 698 (1979).

6) W.A.Lanford and J.F.Ziegler, Experiment Proposal 79-141 to IUCF.

7) J.P.Alard, A.Baldit, R.Brun, J.P.Costilhes, J.Dhermain, J.Farqeix, L.Fraysse, J.Pellet, G.Roche, J.C.Tamain, A.Cordaillat, and A.Pasinetti, Nuovo Cimento 30A, 320 (1975).

8) G.D.Westfall, R.G.Sextro, A.M.Poskanzer, A.M.Zebelman, G.W.Butler and E.K.Hyde, Phys. Rev. C17, 1368 (1978).

9) J.C.Corriso, F.Schlepuetz and K.O.H.Ziock, Nucl. Instr. 133, 121, (1976).

10) M.L.Johnson, J.L.Romero, T.S.Subramanian and F.P.Brady, Nucl. Instr. 169, 179, (1980).

11) F.S.Goulding, D.A.Landis, J.Ceray III and R.H.Pehl, IEEE Trans. Nucl. Sc. NS-13, 514, (1960).

12) J.B.Marion and F.C.Young, Nuclear Reaction Analysis, North-Holland Publishing Co., New York, N.Y., (1968).

13) L.C.Northcliffe and R.F.Schilling, Nuclear Data Tables, A7, 233, (1970).

14) G.Brooke, Cosmic Rays at Ground Level, The Institute of Physics, London, England, 57, (1973).

15) E.Segrè, Nuclei and Particles, Second Edition, W.A.Benjamin Inc., 509, (1977).

16) H.Enge, Introduction to Nuclear Physics, Addison-Wesley Publishing Co., 51, (1966).